

NASA/TM-2014-218148



Current Performance Characteristics of NASA Langley Research Center's Cockpit Motion Base and Standardized Test Procedure for Future Performance Characterization

*Brandon Cowen and Mary T. Stringer
Adaptive Aerospace Group, Inc., Hampton, Virginia*

*Brian K. Hutchinson, Paul C. Davidson, and Lawrence E. Gupton
Langley Research Center, Hampton, Virginia*

NASA STI Program . . . in Profile

Since its founding, NASA has been dedicated to the advancement of aeronautics and space science. The NASA scientific and technical information (STI) program plays a key part in helping NASA maintain this important role.

The NASA STI program operates under the auspices of the Agency Chief Information Officer. It collects, organizes, provides for archiving, and disseminates NASA's STI. The NASA STI program provides access to the NASA Aeronautics and Space Database and its public interface, the NASA Technical Report Server, thus providing one of the largest collections of aeronautical and space science STI in the world. Results are published in both non-NASA channels and by NASA in the NASA STI Report Series, which includes the following report types:

- **TECHNICAL PUBLICATION.** Reports of completed research or a major significant phase of research that present the results of NASA Programs and include extensive data or theoretical analysis. Includes compilations of significant scientific and technical data and information deemed to be of continuing reference value. NASA counterpart of peer-reviewed formal professional papers, but having less stringent limitations on manuscript length and extent of graphic presentations.
- **TECHNICAL MEMORANDUM.** Scientific and technical findings that are preliminary or of specialized interest, e.g., quick release reports, working papers, and bibliographies that contain minimal annotation. Does not contain extensive analysis.
- **CONTRACTOR REPORT.** Scientific and technical findings by NASA-sponsored contractors and grantees.

- **CONFERENCE PUBLICATION.** Collected papers from scientific and technical conferences, symposia, seminars, or other meetings sponsored or co-sponsored by NASA.
- **SPECIAL PUBLICATION.** Scientific, technical, or historical information from NASA programs, projects, and missions, often concerned with subjects having substantial public interest.
- **TECHNICAL TRANSLATION.** English-language translations of foreign scientific and technical material pertinent to NASA's mission.

Specialized services also include organizing and publishing research results, distributing specialized research announcements and feeds, providing information desk and personal search support, and enabling data exchange services.

For more information about the NASA STI program, see the following:

- Access the NASA STI program home page at <http://www.sti.nasa.gov>
- E-mail your question to help@sti.nasa.gov
- Fax your question to the NASA STI Information Desk at 443-757-5803
- Phone the NASA STI Information Desk at 443-757-5802
- Write to:
STI Information Desk
NASA Center for AeroSpace Information
7115 Standard Drive
Hanover, MD 21076-1320

NASA/TM-2014-218148



Current Performance Characteristics of NASA Langley Research Center's Cockpit Motion Base and Standardized Test Procedure for Future Performance Characterization

*Brandon Cowen and Mary T. Stringer
Adaptive Aerospace Group, Inc., Hampton, Virginia*

*Brian K. Hutchinson, Paul C. Davidson, and Lawrence E. Gupton
Langley Research Center, Hampton, Virginia*

National Aeronautics and
Space Administration

Langley Research Center
Hampton, Virginia 23681-2199

January 2014

ACKNOWLEDGMENTS

Special thanks are extended to the many people that contributed to the extensive testing and evaluation process during the development of this report. This effort would not have been possible without the guidance and assistance of Fred Lallman, Robert Redman, Dale Ashcom, and Gustav Taylor of the NASA Langley Research Center, Keith Hoffler of Adaptive Aerospace Group, as well as Frank Cardullo of the State University of New York- Binghamton.

The use of trademarks or names of manufacturers in this report is for accurate reporting and does not constitute an official endorsement, either expressed or implied, of such products or manufacturers by the National Aeronautics and Space Administration.

Available from:

NASA Center for AeroSpace Information
7115 Standard Drive
Hanover, MD 21076-1320
443-757-5802

NOMENCLATURE

Symbols

CMB	Cockpit Motion Base
CMF	Cockpit Motion Facility
DCU	Digital Control Unit
DoF	Degree-of-Freedom
DVS	Data Visualization System
GFD	Generic Flight Deck
IFD	Integration Flight Deck
PSD	Power Spectral Density
RFD	Research Flight Deck
SDAB	Simulation Development and Analysis Branch
SID	System Identification
SIMES	SIMulator Evaluation System

Table of Contents

NOMENCLATURE	iii
LIST OF FIGURES	v
INTRODUCTION	2
CMB MOTION SYSTEM CONFIGURATION	4
DIGITAL CONTROL LAW	4
CMB Parasitic Accelerations- Past and Present	5
Control Law Modification	7
CMB PERFORMANCE AND COMPARISONS	9
Transport Delay	9
Performance Test Input Signals	10
Performance Characteristics	12
CMF STANDARDIZED TESTING PROTOCOL	21
Standard Spectral Inputs	21
Chirp Inputs	21
Banked, Sinusoidal Inputs	22
Standard Test Procedure	23
Standard Post-Processing Tools	23
Automated Processing Scripts	23
Graphical User Interface (GUI)	23
Additional Functions	24
CONSIDERATIONS	24
CONCLUSIONS	25
BIBLIOGRAPHY	26
APPENDIX	27
Comparison of Production Controller to Previous Controller	27

LIST OF FIGURES

Figure 1: GFD interior (left) and exterior on CMB (right)	2
Figure 2: CMF representation showing the CMB, available cabs, and the crane	3
Figure 3: Control architecture for the CMB.....	3
Figure 4: Cab-axes coordinate frame	4
Figure 5: Uncommanded motion and residual motion for 0.45 inch- 4Hz sinusoid Leg 1 position command.....	6
Figure 6: Uncommanded motion during 1 inch- 2Hz sinusoid level heave command	6
Figure 7: Leg target-velocity test results.....	7
Figure 8: Parasitic accelerations during increasing banked heave oscillations.....	8
Figure 9: System latency test using SIMES with 10kHz sampling rate- 20 sec step input to Leg 5.	10
Figure 10: Time history of commanded frequency sweep.....	11
Figure 11: Power Spectral Density of commanded frequency sweep.....	12
Figure 12: Bode Plot for Production Controller - Heave	13
Figure 13: Bode Plot for Production Controller - Sway	13
Figure 14: Bode Plot for Production Controller – Surge	14
Figure 15: Bode Plot for Production Controller – Pitch	14
Figure 16: Bode Plot for Production Controller – Roll.....	15
Figure 17: Bode Plot for Production Controller – Yaw	15
Figure 18: Production Controller - Parasitic Acceleration from Commanded Heave (dB)	16
Figure 19: Production Controller - Parasitic Acceleration from Commanded Pitch (dB)	17
Figure 20: Production Controller - Parasitic Acceleration from Commanded Roll (dB)	17
Figure 21: Production Controller - Parasitic Acceleration from Commanded Surge (dB).....	18
Figure 22: Production Controller - Parasitic Acceleration from Commanded Yaw (dB).....	18
Figure 23: Production Controller - Parasitic Acceleration from Commanded Sway (dB)	19
Figure 24: Operational Limits (Heave).....	20
Figure 25: Operational Limits (Sway)	20
Figure 26: Operational Limits (Banked Heave).....	21
Figure 27: Sample sweave-spline time history	22
Figure 28: GUI - Post Processing Tool.....	24
Figure 29: CMB valve performance	25
Figure 30: Bode Plot Comparison – Heave	27
Figure 31: Bode Plot Comparison – Sway.....	27

Figure 32: Bode Plot Comparison – Surge	28
Figure 33: Bode Plot Comparison – Pitch	28
Figure 34: Bode Plot Comparison – Roll.....	29
Figure 35: Bode Plot Comparison – Yaw	29
Figure 36: Previous Controller - Parasitic Acceleration from Commanded Heave (dB).....	30
Figure 37: Previous Controller - Parasitic Acceleration from Commanded Pitch (dB).....	30
Figure 38: Previous Controller - Parasitic Acceleration from Commanded Roll (dB).....	31
Figure 39: Previous Controller - Parasitic Acceleration from Commanded Surge (dB)	31
Figure 40: Previous Controller - Parasitic Acceleration from Commanded Sway (dB).....	32
Figure 41: Previous Controller - Parasitic Acceleration from Commanded Yaw (dB)	32
Figure 42: Previous Controller – Cross-coupled acceleration gains by increasing cab roll angle.	33

ABSTRACT

This report documents the updated performance characteristics of NASA Langley Research Center's (LaRC) Cockpit Motion Base (CMB) after recent revisions that were made to its inner-loop, feedback control law. The modifications to the control law will be briefly described. The performance of the CMB will be presented. A short graphical comparison to the previous control law can be found in the appendix of this report. The revised controller will be shown to yield reduced parasitic accelerations with respect to the previous controller. Metrics based on the AGARD Advisory Report No. 144 are used to assess the overall system performance due to its recent control algorithm modification. This report also documents the standardized simulator test procedure which can be used in the future to evaluate potential updates to the control law.

INTRODUCTION

The Cockpit Motion Facility (CMF) located at the NASA Langley Research Center (LaRC) contains a 6 degree-of-freedom (6-DOF) motion platform with three interchangeable operational flight simulator cockpits, also referred to as cabs, as well as a crane to reposition the cabs. The Cockpit Motion Base (CMB) is operated and maintained by LaRC's Simulation Development and Analysis Branch (SDAB), providing NASA, DoD and many other institutions and companies a state-of-the-art synergistic motion platform for aerospace research. This report aims to quantify the current operational performance of the motion system and discuss a standardized performance test procedure method. The procedure and tools outlined were used in determining the performance characteristics presented. In addition, the motivation for the recent control law modification is discussed. The characteristics of the previous controller, which was actively used on the CMB until October 2012, are provided in the appendix for comparison purposes only. This report will also briefly document the system architecture of the facility, describing the modification of commanded accelerations from a host simulation as they are filtered, transformed, and finally sent to drive the platform.



Figure 1: GFD interior (left) and exterior on CMB (right)

The CMB features six 76-inch leg stroke extension low-friction hydrostatic bearing actuators in a hexapod configuration. The facility currently has three operational cabs that can be placed on the motion base for motion testing or operated in a fixed-based environment independent of the motion base. Cabs are transferred from their fixed-base locations to the motion platform via an overhead facility crane system and lifting rig. The three cabs are the Research Flight Deck Simulator cab (RFD), the Generic Flight Deck Simulator cab (GFD)- seen in Figure 1, and the Integration Flight Deck Simulator cab (IFD). There is a fourth cab dock station available for future acquisition of an additional cab. Figure 2 contains a graphic of the overall facility.



Figure 2: CMF representation showing the CMB, available cabs, and the crane

The performance characteristics of the motion system are continuously being defined by the SDAB. Through systematic testing, the branch is expending effort to further define the current state of performance as well as implement modifications in the software to improve the performance. The basis of the performance metrics and the subsequent determination of the platform characteristics are compiled from Reference [1] and based on AGARD-AR-144 [2]. AGARD-144 documents methodologies for evaluating the motion platform via time and frequency domain characterization techniques, along with assessments of acceleration noise and parasitic acceleration. Parasitic acceleration as defined in [2] is the resulting measured acceleration in the “undriven” degrees-of-freedom occurring when accelerations are commanded in another “driven” degree-of-freedom. Current literature also refers to this phenomena as cross-coupling, or cross-talk.

This report defines a systematic method for measuring the dynamic qualities of simulator motion systems. Numerous simulators have been evaluated with the methodologies defined in AGARD-144, including the SIMONA Research Simulator at Delft University of Technology [3] and the Visual Motion Simulator at NASA LaRC. The AGARD-144 report has also been used as the basis for assessments of the relationship between motion base performance and pilot perception[2].

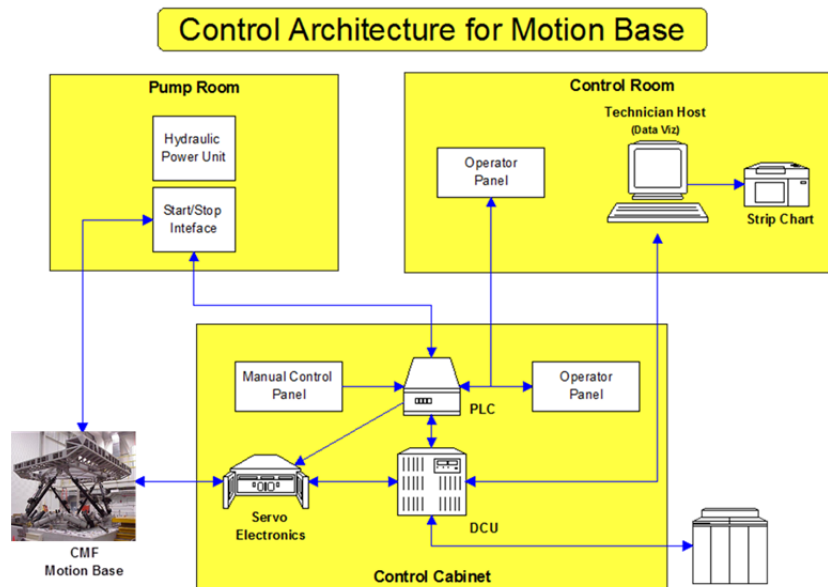


Figure 3: Control architecture for the CMB

CMB MOTION SYSTEM CONFIGURATION

The CMB relies on an integrated network for command and control. Figure 3 illustrates the primary systems involved in passing motion commands and processing feedback from the motion base. A typical research experiment would involve a host computer with a 6DoF aircraft simulation passing acceleration commands to the digital control unit (DCU). The DCU contains the digital control law (DCL) necessary for processing and commanding the desired motion base trajectory. The resulting position commands are then converted to an analog signal commanding two valves per leg to achieve a desired leg extension/retraction. Note that the two valves connected to a single leg receive identical commands. The resulting coordinated leg position adjustment transports the motion base and cab to a new translational and rotational orientation. Position and velocity of each leg are measured and fed back to the DCU/DCL as an analog signal which is then sampled at 2kHz in the internal feedback loop. This feedback loop is separate from the aircraft simulation providing commands from the host computer, which would typically be running at <100 Hz. The platform has a set of accumulators designed to sustain hydraulic system pressure by providing supplemental flow during periods of high demand, and subsequently to recharge while the extra pressure is not needed.

All measurements provided in this paper will be defined relative to a simulator reference frame which is depicted in Figure 4. The remaining degrees-of-freedom are the typical roll, pitch and yaw attitudes defined in the same manner as traditional aircraft Euler angles. This coordinate system is defined in more detail in [4]. Also, note that the general orientation of the six hydraulic actuators is also shown in Figure 4.

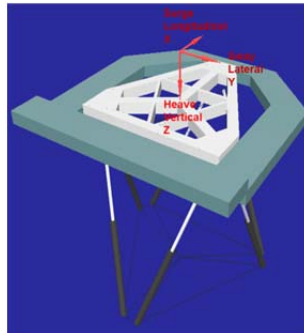


Figure 4: Cab-axes coordinate frame

The motion centroid excursion limits in the previously defined simulator coordinate are shown in Table 1. These limits are representative of the absolute position limits of the system. It should be noted, however, that multiple extremities of the excursion envelope are not realistically attainable at the same time due to geometric constraints.

DIGITAL CONTROL LAW

The signal to noise ratio of a motion base system, as suggested in [2], dictates the operational capabilities of a motion base simulator. As with all nonlinear mechanical systems of this type, some level of off-axis acceleration noise occurs naturally and degrades the operational capabilities. The control law of the CMB was recently modified to reduce the presence of parasitic accelerations. The recent revision to the motion base's inner-loop control focused on reducing the CMB's off-axis acceleration noise otherwise known as parasitic accelerations. The resulting revision was implemented to promote as much symmetry in the leg performance as possible.

Table 1: DoF excursion capability [3]

Degree of Freedom	Commanded	Measured	Difference
Surge (inch)	67	67.88	0.88
	-55	-53.94	-1.06
Sway (inch)	55	54.50	-0.50
	-55	-54.50	-0.50
Heave (inch)	41	41.30	0.30
	-41	-40.00	-1.00
Yaw (degree)	38	36.27	-1.73
	-38	-36.52	-1.48
Pitch (degree)	28	27.30	-0.70
	-25	-25.30	0.30
Roll (degree)	28	28.10	0.10
	-28	-28.00	0.00

CMB Parasitic Accelerations- Past and Present

Parasitic acceleration is defined relative to the simulator reference frame, however, for analysis, it is often convenient to analyze individual leg responses with positive or negative excursion defined relative to the orientation of the legs. Therefore, the resulting axes are constantly moving as the legs extend and retract. Figure 5 shows the time history of a run where the commanded extension of a single leg was a constant frequency sinusoid, while the commanded extensions of the five other legs were zero. The top subplot in Figure 5 shows the commanded motion of the single leg, and the resulting uncommanded movement of the remaining five legs. As differential piston pressure is continuously measured and piston area is known, the forces in each leg are computed for the same time series of data and plotted in the bottom subplot. For an approximately 17,000 lb (8.5 ton) cab such as the GFD, the required forces to simply prevent the five “resting” legs from moving are quite significant.

Leaving the leg position perspective, Figure 6 shows simulator reference frame heave position commanded in the form of a constant frequency sinusoidal wave with a +/- 1 inch peak amplitude. The resulting commanded positions in the illustrate the real-world impact of the parasitic accelerations. Uncommanded motion in the sway and surge degrees of freedom are clearly noticeable, in addition to much smaller displacements in all three rotational degree of freedoms, which are seen in the zoomed snapshot.

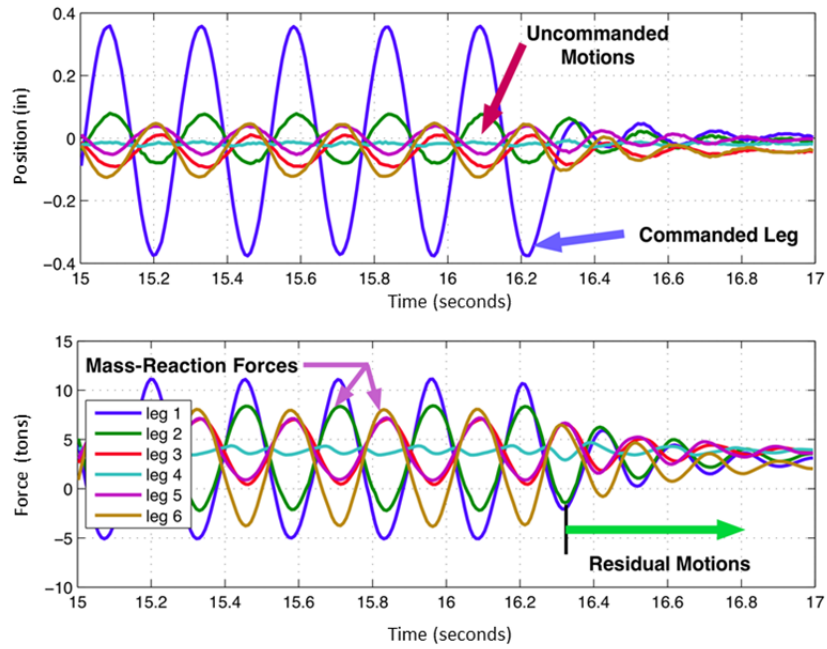


Figure 5: Uncommanded motion and residual motion for 0.45 inch- 4Hz sinusoid Leg 1 position command.

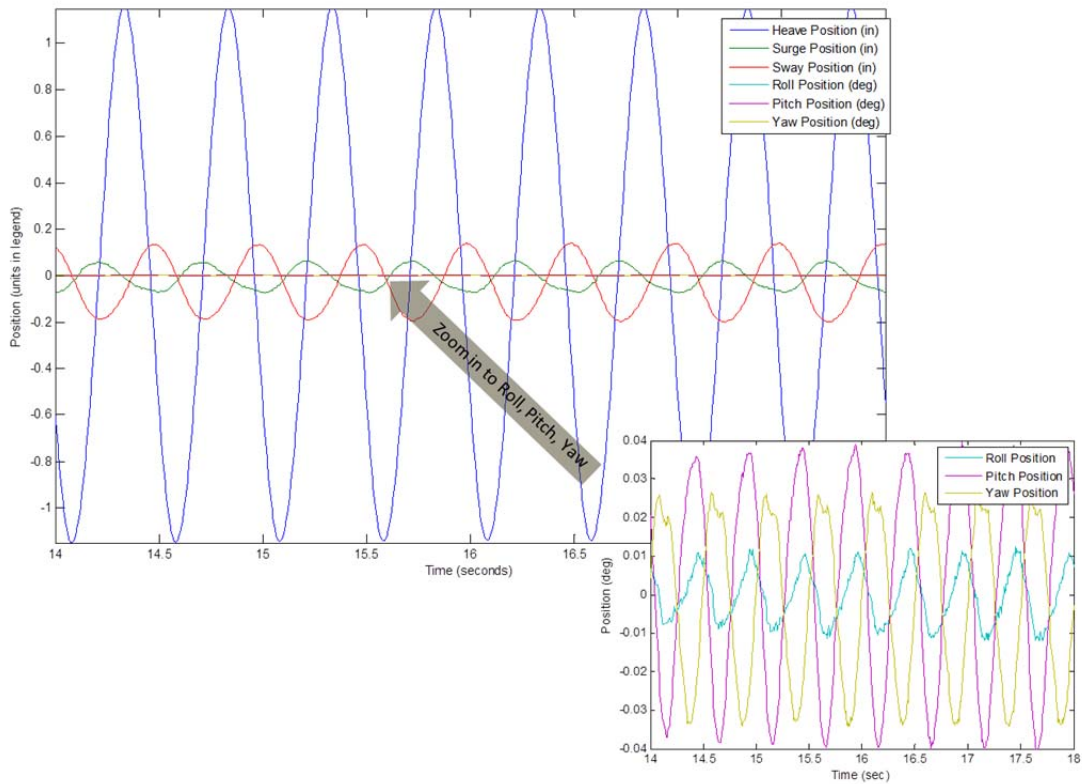


Figure 6: Uncommanded motion during 1 inch- 2Hz sinusoid level heave command

Control Law Modification

CMB testing showed that not all legs, and more specifically their valves, were performing equally. Figure 7 demonstrates the velocity output of each of the six legs for both extend and retract with respect to valve command, where valve command represents the input to each leg. The valve command for each leg is passed to two valves, as each leg utilizes two valves, resulting in twice the total leg velocity for each maneuver. While the performance of the six legs closely match in extension- positive valve commands, there is a wider range in performance of the legs during retraction- negative valve commands. The valves were tested to +/- 80% (green region) and linearly extrapolated to generate the higher valve command percentages (pink region).

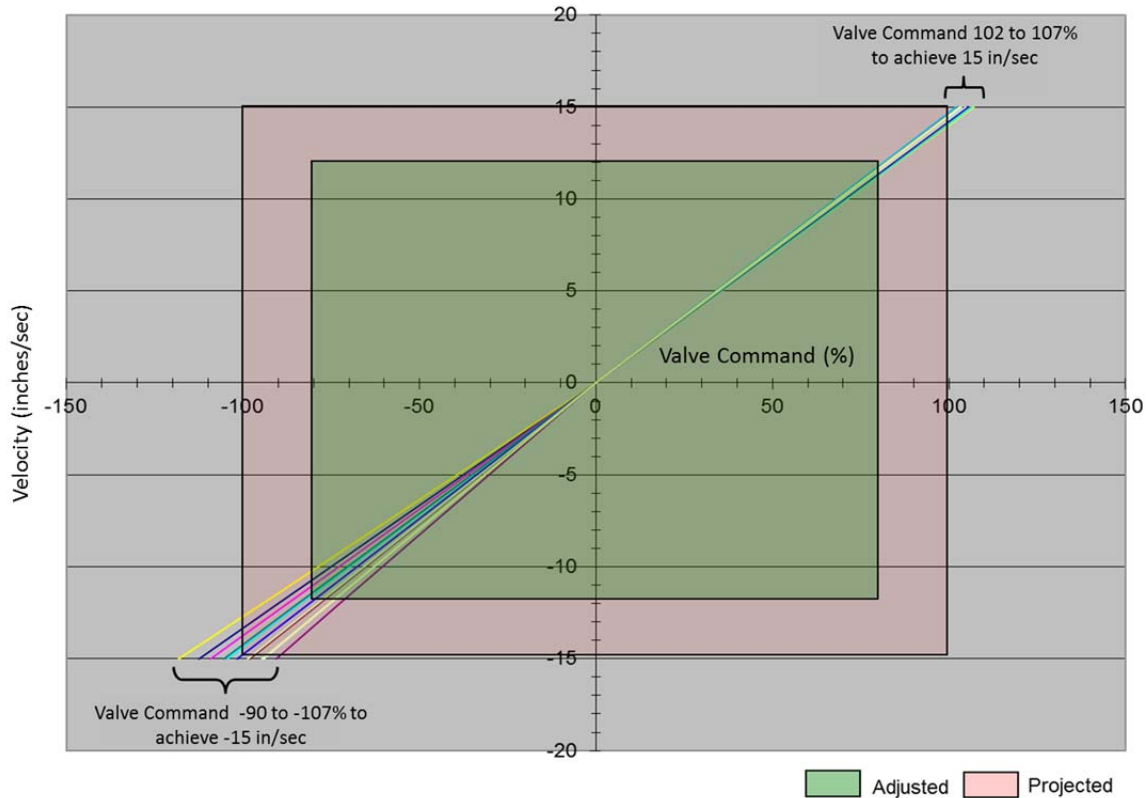


Figure 7: Leg target-velocity test results

To address this occurrence, a gain was added in the control law to the retract command of the five faster retracting legs to reduce the commanded valve position and slow their retraction to the retract velocity of the slowest leg. The resulting modification resulted in reduced parasitic accelerations. Figure 8 presents the response of the CMB with the GFD cab during banked motion. To assess the parasitic acceleration in the sway axis, the motion base was banked to several orientations with sinusoidal accelerations commanded in cab-axis heave. The commanded simulator reference frame pure heave motion consisted of constant frequency sinusoids ranging from 0.5Hz to 4Hz, in increments of 0.5Hz, splined together after two cycles at each frequency. The measured simulator reference frame heave and sway accelerations in Figure 8 illustrate the levels of parasitic (sway in this example) accelerations across several frequencies for both the previous and new production control laws. Significant reduction in the parasitic sway accelerations was achieved. The overall performance of the new production controller is presented in the following section. For comparison, the performance characteristics of the previous controller are provided in the Appendix.

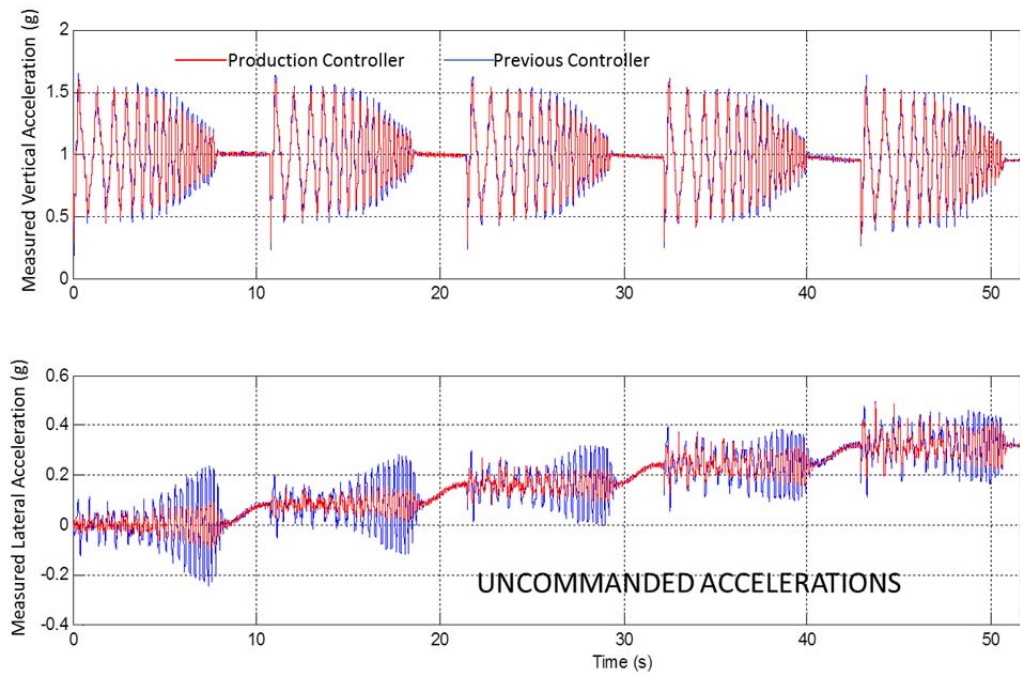


Figure 8: Parasitic accelerations during increasing banked heave oscillations

CMB PERFORMANCE AND COMPARISONS

The motion base performance is presented mostly from a linear analysis perspective. All results represent the performance of the motion base with the GFD cab. The additional cabs, the IFD and RFD, have different masses and weight distributions- Table 2. Note that the CG information is provided in body , specifically simulator, reference frame. Despite these differences, the performance of the motion base with these cabs is expected to be comparable.

PAYLOAD MASS CHARACTERISTICS from NASTRAN	
GFD Properties:	
Total Mass	+33342.31570 (lbm)
CG Position	x = -2.90 y = -0.11 z = -31.20 (in)
CG Force	x = 0.00 y = 0.00 z = -33342.26 (lbf)
CG Moment	x = 0.00 y = 0.00 z = 0.00 (lbf-in)
Inertia Moments (CG)	Ixx = +433077.8 Iyy = +424668.4 Izz = +666520.0 (lbf-in-sec ²)
Inertia Products (CG)	Ixy = +433.6 Iyz = -126.8 Ixz = +5275.6 (lbf-in-sec ²)
RFD Properties:	
Total Mass	+36329.90904 (lbm)
CG Position	x = -3.47 y = -0.19 z = -41.58 (in)
CG Force	x = 0.00 y = 0.00 z = -36329.85 (lbf)
CG Moment	x = 0.00 y = 0.00 z = 0.00 (lbf-in)
Inertia Moments (CG)	Ixx = +595489.7 Iyy = +588245.7 Izz = +735953.7 (lbf-in-sec ²)
Inertia Products (CG)	Ixy = -1008.8 Iyz = +107.5 Ixz = +17987.6 (lbf-in-sec ²)
IFD Properties:	
Total Mass	+36641.73343 (lbm)
CG Position	x = -4.35 y = -0.44 z = -41.60 (in)
CG Force	x = 0.00 y = 0.00 z = -36641.67 (lbf)
CG Moment	x = 0.00 y = 0.00 z = 0.00 (lbf-in)
Inertia Moments (CG)	Ixx = +595191.9 Iyy = +588097.2 Izz = +735931.1 (lbf-in-sec ²)
Inertia Products (CG)	Ixy = +807.5 Iyz = +395.6 Ixz = +18097.5 (lbf-in-sec ²)

Table 2. Payload Mass Characteristics

The characterization effort focuses on the transport delay, or time delay, between simulation command and first measured motion was detected, as well as the frequency response in all 6DoFs. Because this recent control law modification aimed to reduce the parasitic accelerations, the frequency response of the off-axis accelerations are also presented.

Transport Delay

The transport delay of a single leg on the motion base was measured using SIMES, a simulator instrumentation measurement system, as approximately 25 +/- 8ms. The results are depicted in Figure 9.

The four signals in this figure represent both the position and velocity feedback signal on the leg, as well as the two separate valve commands supporting that leg, ISVA- Valve Command A and ISVB- Valve Command B. ISV(A&B) are the servovalve drive currents measured across an internal shunt resistor. The test was conducted with a step commanded directly from the DCU and processed by taking measurements of first valve movement (position and velocity). Measuring first motion of the physical motion platform is of course limited by sensor sensitivity which has not been quantified or included.

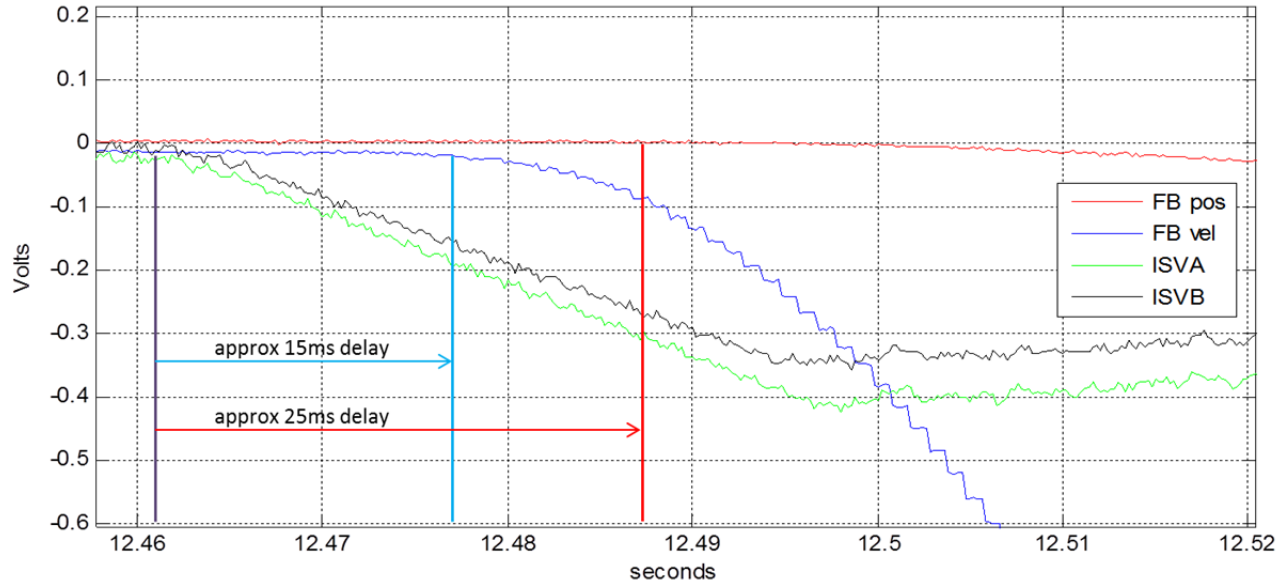


Figure 9: System latency test using SIMES with 10kHz sampling rate- 20 sec step input to Leg 5.

Performance Test Input Signals

Linear analysis of CMB/GFD's dynamic response was performed with commanded frequency sweeps. Sinusoidal input signals are preferred for performance analysis over impulses, steps and ramps due to their similarity to normal aircraft control inceptor inputs [4, 5].

$$f_i(t) = f_0(t_i) + \left[\frac{f_i(t_f) - f_0}{t_f} \right] t \quad (1)$$

The frequency sweep, or chirp signal, used for testing is shown in Figure 10 and given by Equation 1 [7]. Note that the bottom subplot of this figure is a zoomed snapshot of the acceleration command. The chirp signal was designed to minimize unnecessary violent accelerations on the system across the tested frequency ranges. For this reason, extensive testing with constant frequency sinusoids sweeping through a broad range of frequencies was rejected. This chirp signal is relatively short in duration. However, the results show adequate information for frequency domain analysis. The chirp signal commands simulator reference frame position, velocity, and acceleration. The chirp signal linearly sweeps through frequencies 0.05 Hz, $f_0(t_i)$, to 7 Hz, $f_i(t_f)$, at 10ms timesteps.

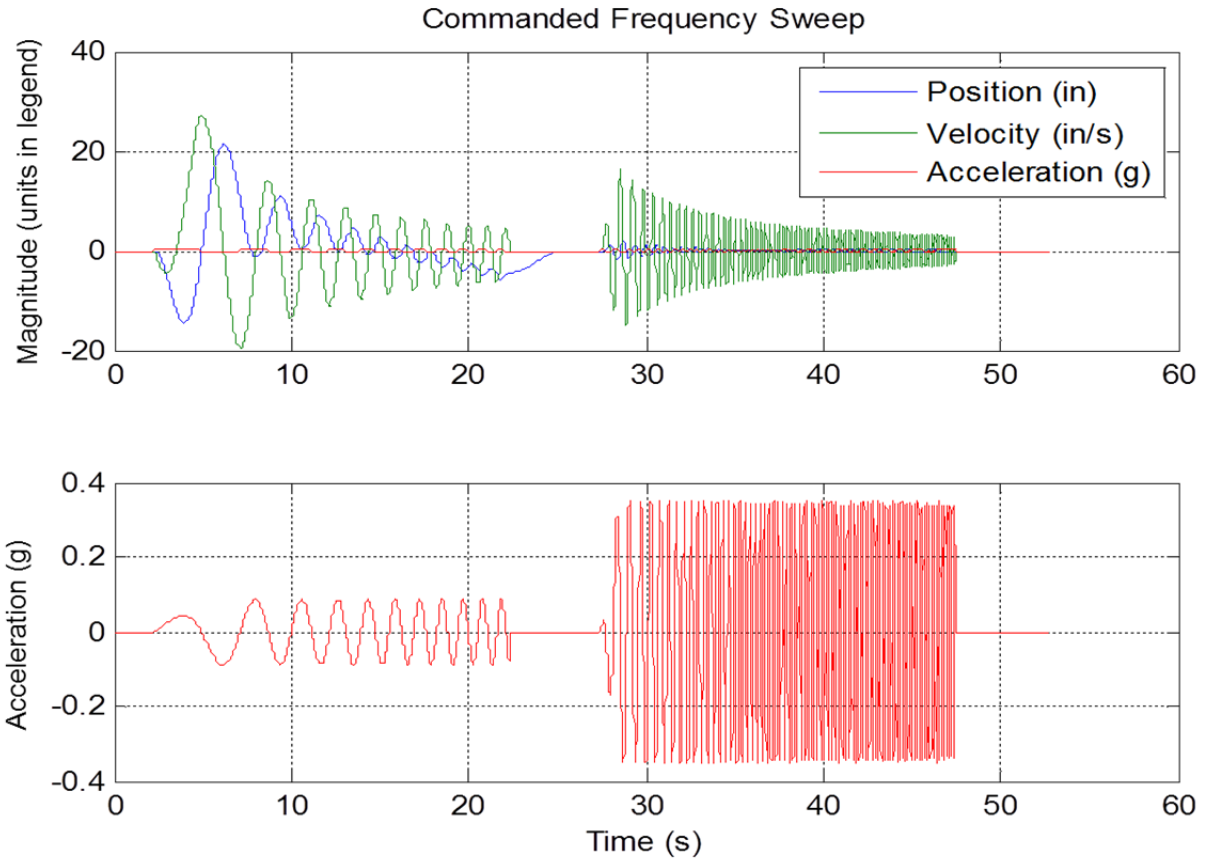


Figure 10: Time history of commanded frequency sweep

The signal was designed to command constant acceleration. To minimize integration errors, the original acceleration command was constructed at 10,000 Hz and then twice integrated to derive the corresponding velocity and position commands. These signals were then downsampled to 100 Hz to achieve the typical command signal frequency. The chirp signal is composed of two segments. The first segment is composed of lower frequencies to reduce the excursion associated with low-frequency, constant-acceleration commands. The first half cycle of each segment is linearly faded-in to reduce initial transients. It should be noted, that while these linear techniques adequately capture the performance of the motion base, there are limitations. Linear frequency domain analysis does not fully represent the system harmonics or other nonlinear dynamics of the system. A primary aspect of the system that is not captured is the fluctuation in performance as the system hydraulic pressure decreases as a result of the accumulators being depleted. The Power Spectral Density (PSD) semilogarithmic plots in Figure 11 show the resulting power of the commanded position and acceleration in decibels across the tested frequency range. In the bottom subplot, note that the drop in power at 1 Hz is most likely due to the windowing around the deadzone of the splined segments of the signal during the Fourier Transform, and not necessarily a lack of frequency content in the chirp at that frequency.

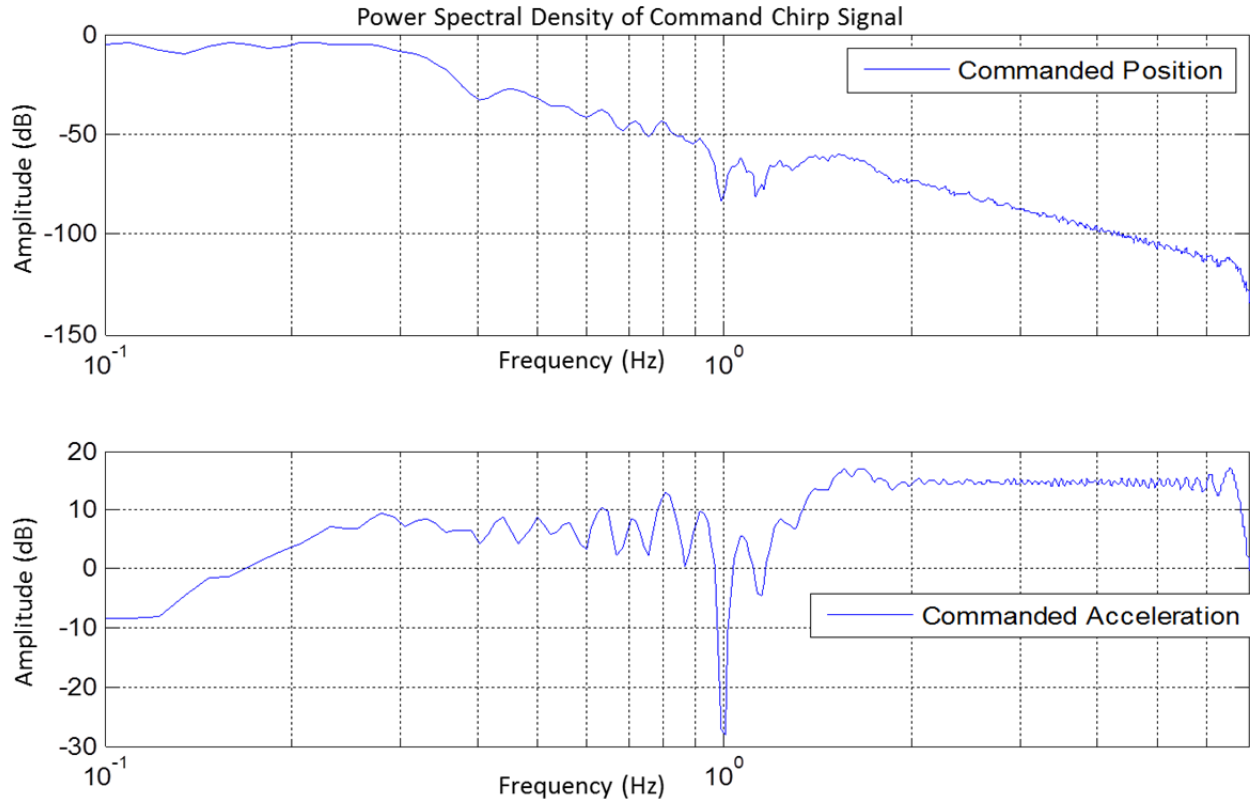


Figure 11: Power Spectral Density of commanded frequency sweep

Performance Characteristics

The performance of the CMB with the GFD cab and the new production control law is presented in Figure 12 through 17. In both the previous and new production control laws, the CMB/GFD achieves a bandwidth approximately to 3 Hz in most degrees of freedom, with phase lag clearly being the limiting factor. The rotational DoFs exhibit a performance roll-off in magnitude as frequency increases. The heave axis behaves in a similar manner while also being the least responsive translation DoF. Surge and sway exhibit appreciable overshoot at higher frequencies, approximately 4 Hz, before sharply falling off in response around 5 Hz. The revised controller does sacrifice some phase margin in all DoFs. However, the closed-loop dynamics of the motion base are not significantly changed in nature. The Bode plots comparing the controllers can be found in the Appendix.

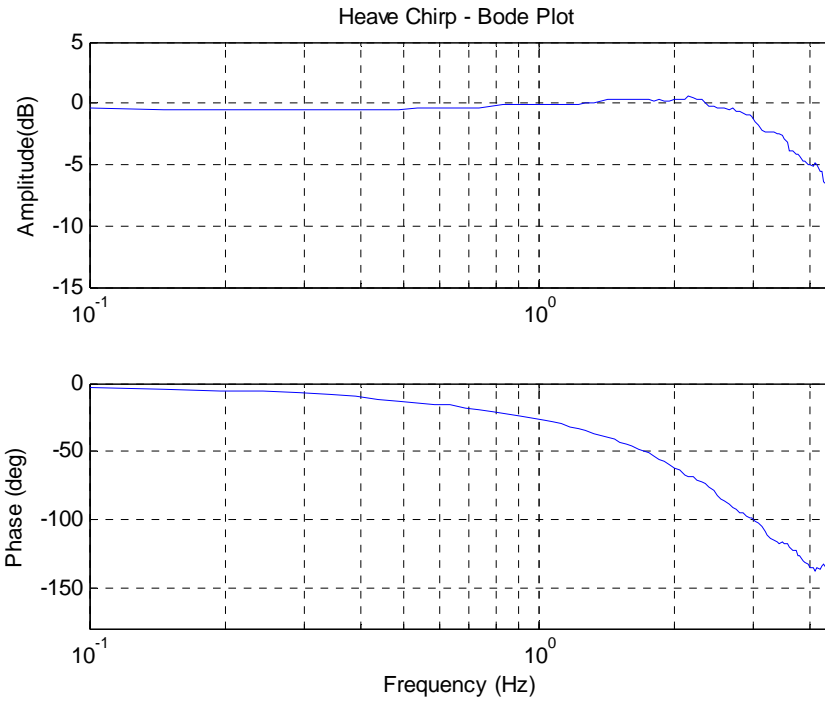


Figure 12: Bode Plot for Production Controller - Heave

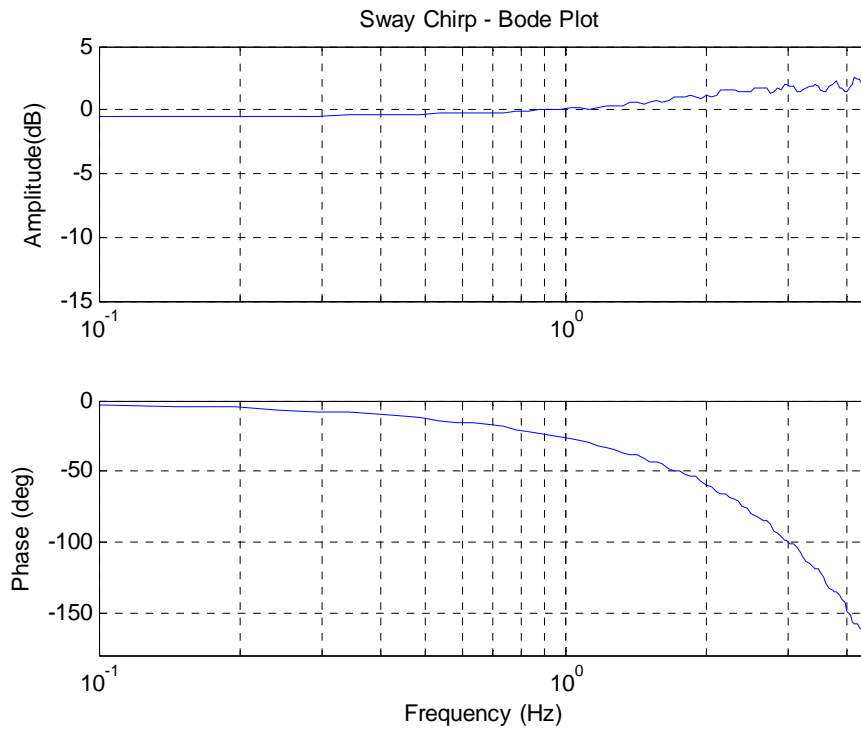


Figure 13: Bode Plot for Production Controller - Sway

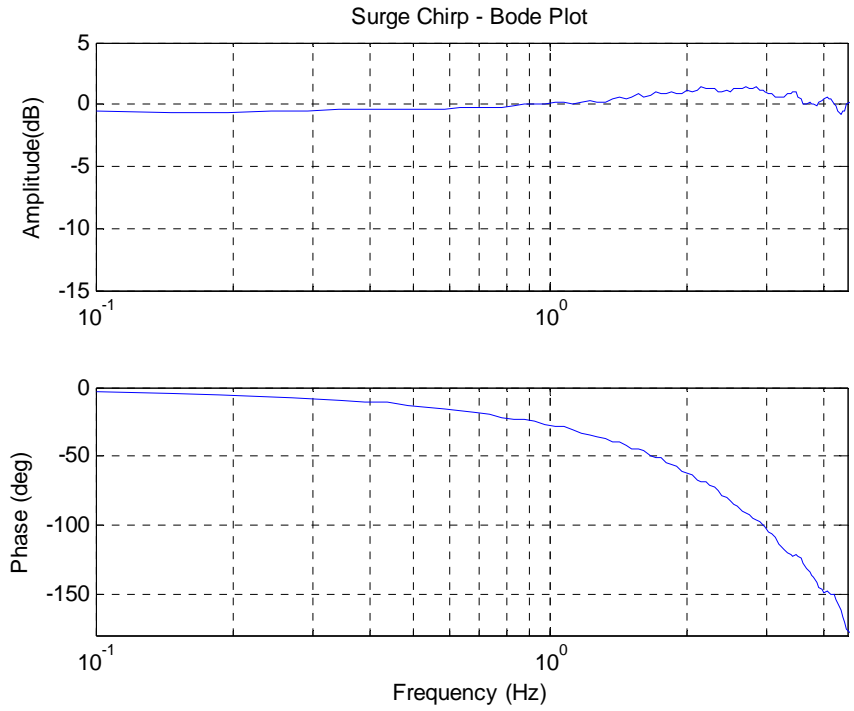


Figure 14: Bode Plot for Production Controller – Surge

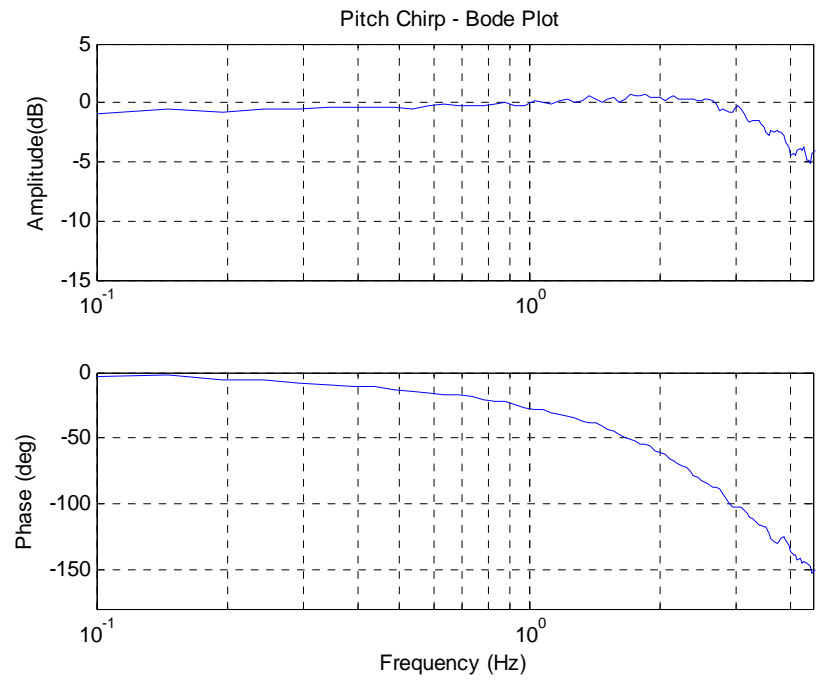


Figure 15: Bode Plot for Production Controller – Pitch

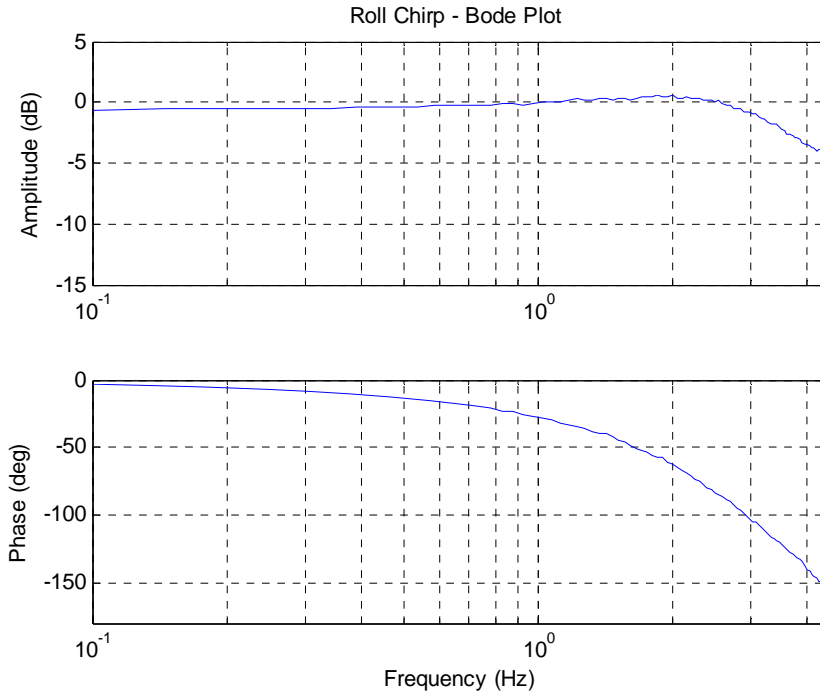


Figure 16: Bode Plot for Production Controller – Roll

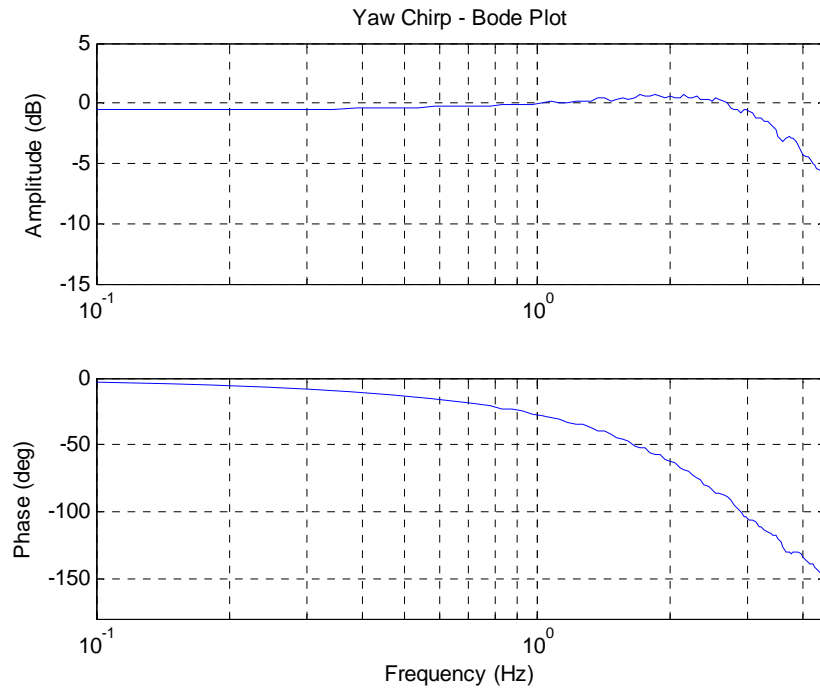


Figure 17: Bode Plot for Production Controller – Yaw

The previous linear analysis techniques were extended to assess the current levels of parasitic acceleration, as this was the motivation for the recent control law modification. The Bode plots in Figures

18 through 23 show the response in all 6 DoFs to a chirp signal commanded in a single DoF. Thus, they represent a total measured response of the parasitic acceleration present in the off-axes. The parasitic accelerations clearly increase with increasing frequency. Moreover, a strong linear correlation with parasitic acceleration and frequency is apparent. Note that neither of the plot axes are linear, so it is not immediately apparent in these plots. This linear trend can be seen in Figure 42 of the Appendix. This 3D figure was generated from testing done with the previous controller and has yet to be duplicated with the current production controller. However, the same trend is expected. Nonlinearities, primarily in the form of apparent harmonics, contribute substantially to the parasitic accelerations in the off-axes. Again, these nonlinearities and their effects cannot be seen in any form of linear analysis.

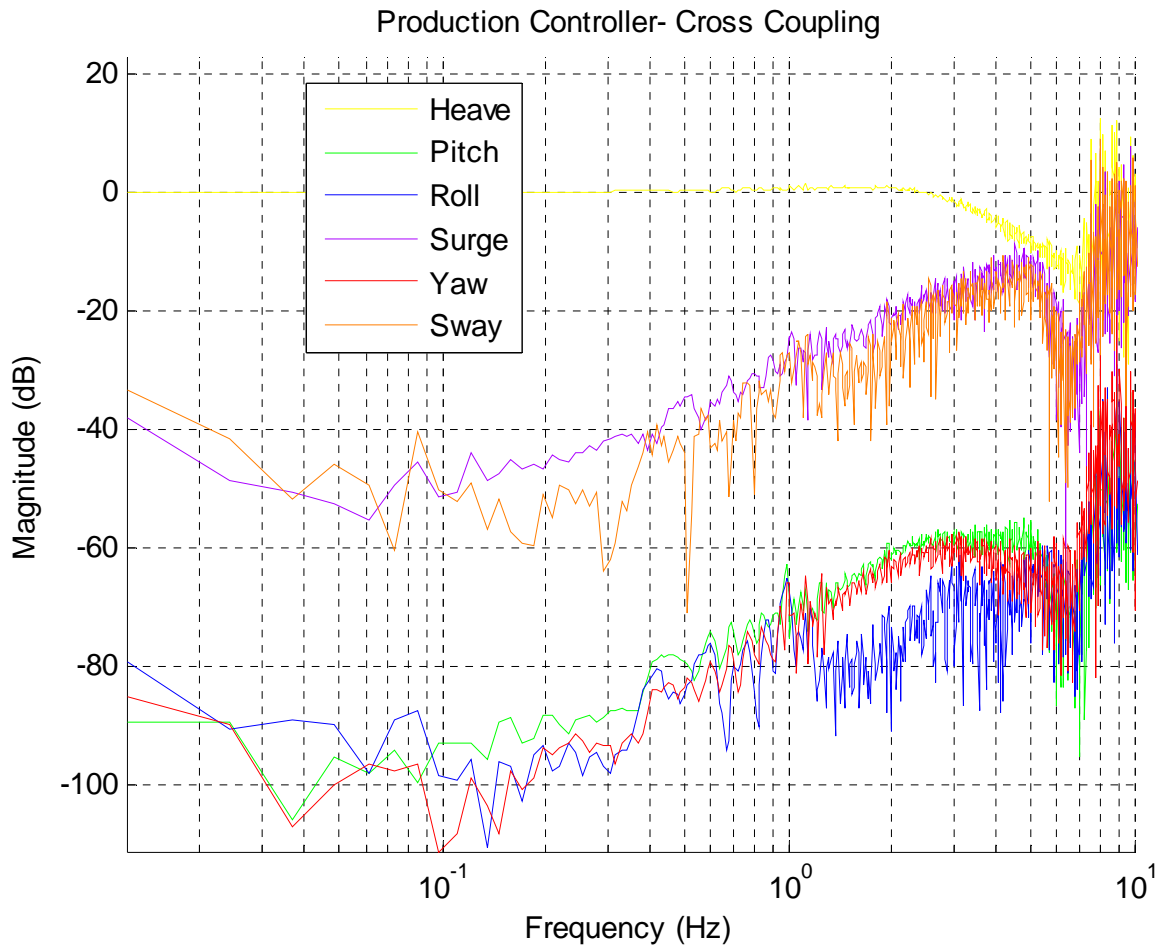


Figure 18: Production Controller - Parasitic Acceleration from Commanded Heave (dB)

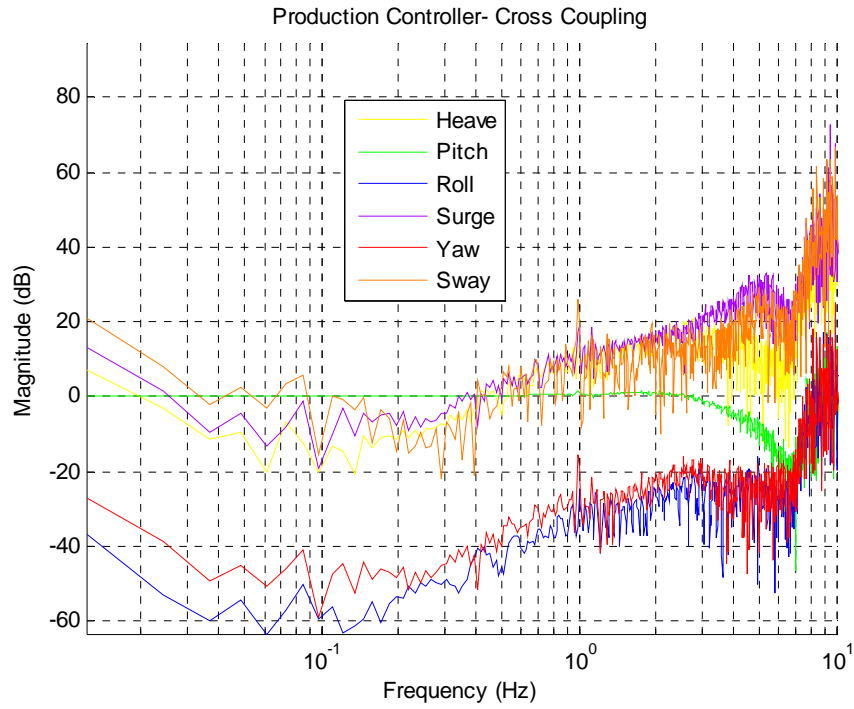


Figure 19: Production Controller - Parasitic Acceleration from Commanded Pitch (dB)

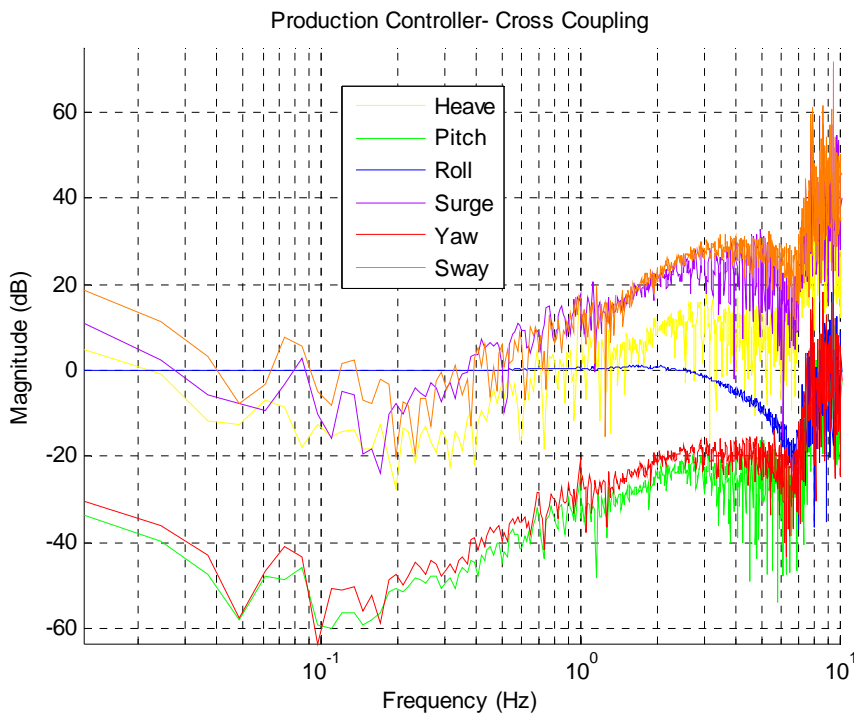


Figure 20: Production Controller - Parasitic Acceleration from Commanded Roll (dB)

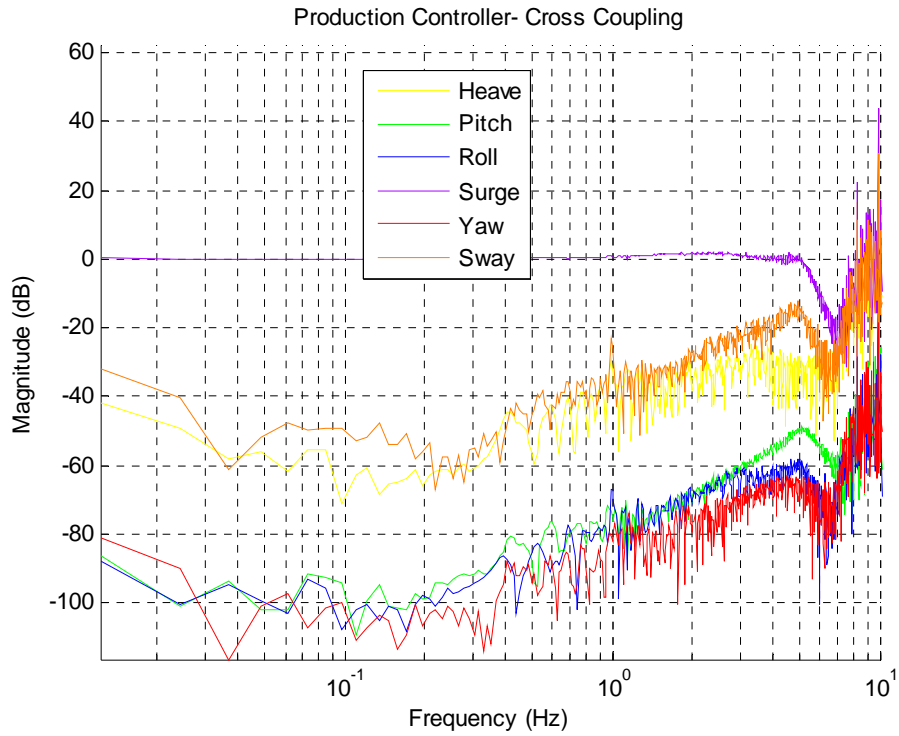


Figure 21: Production Controller - Parasitic Acceleration from Commanded Surge (dB)

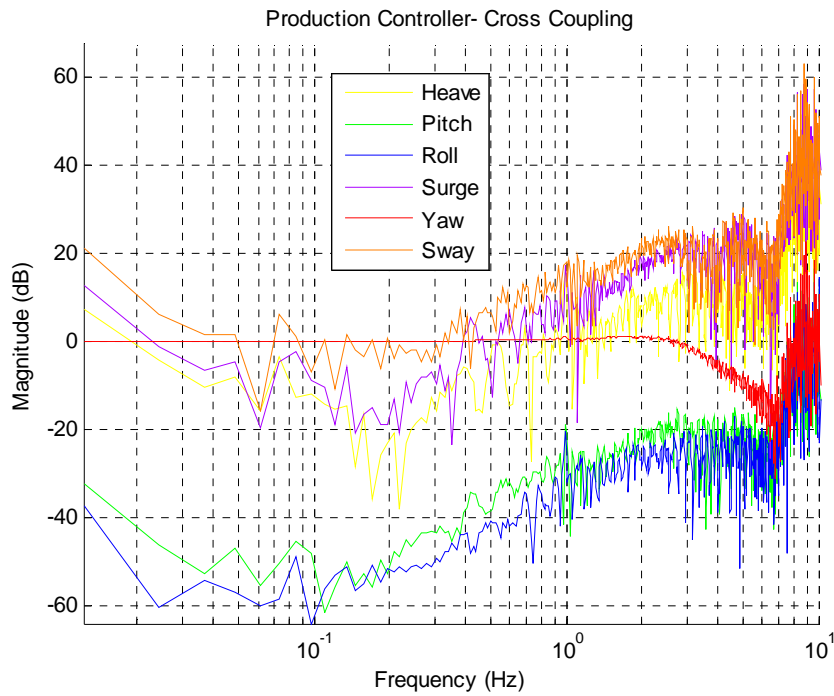


Figure 22: Production Controller - Parasitic Acceleration from Commanded Yaw (dB)

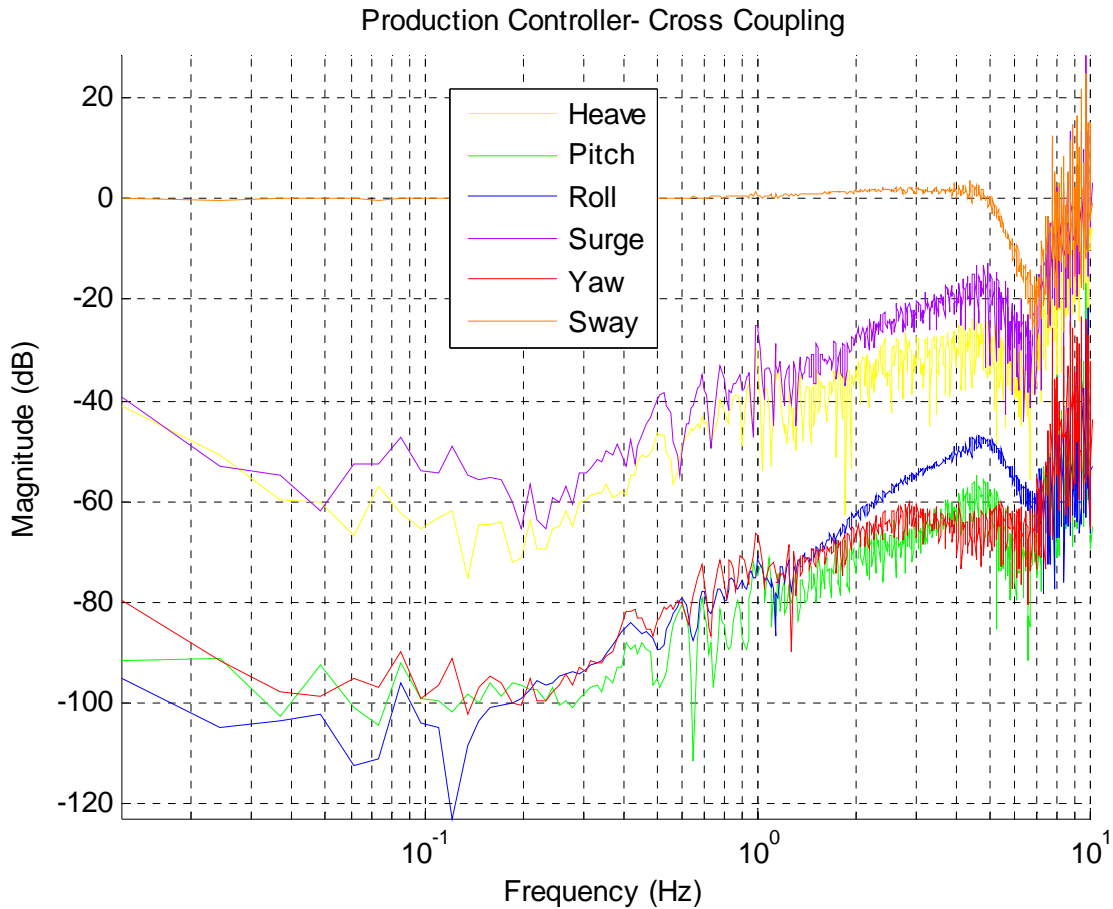


Figure 23: Production Controller - Parasitic Acceleration from Commanded Sway (dB)

Additional information regarding accumulator and pump limits, plotted in the frequency domain, gives more insight into the dynamic operational limits of the platform. Approximate sustained motion capabilities are depicted in Figures 24-26. The CMB/GFD response to commanded heave and sway accelerations is shown in Figure 24 a and Figure 25 respectively. Figure 26 illustrates the limits for commanded heave accelerations with a 15 degree bank angle. The latter figure illustrates the limits during 15 degrees of bank on the off-axis. As previously established, the current closed loop response of the platform peaks near 5 Hz before falling off swiftly. More information regarding the operational limits with regards to CMB safety devices can be found in [9].

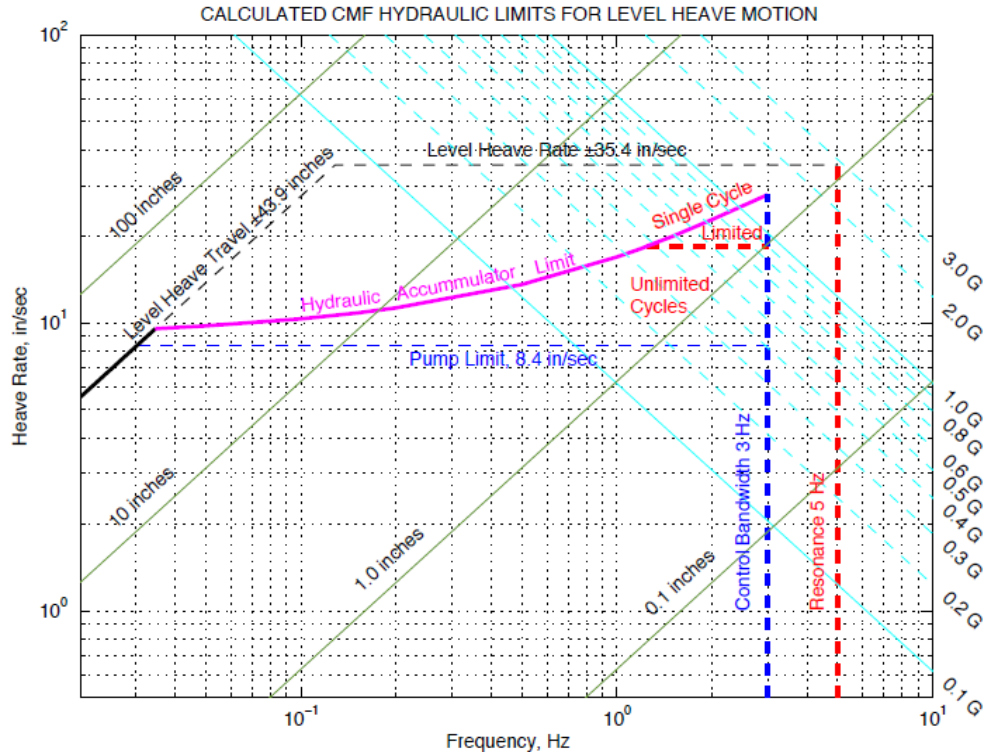


Figure 24: Operational Limits (Heave)

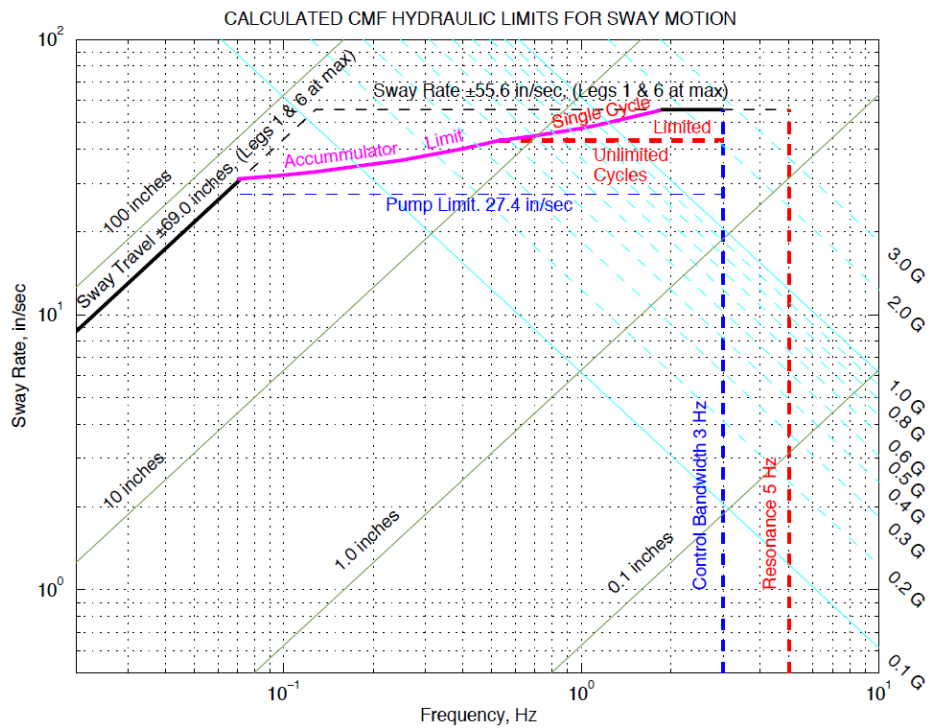


Figure 25: Operational Limits (Sway)

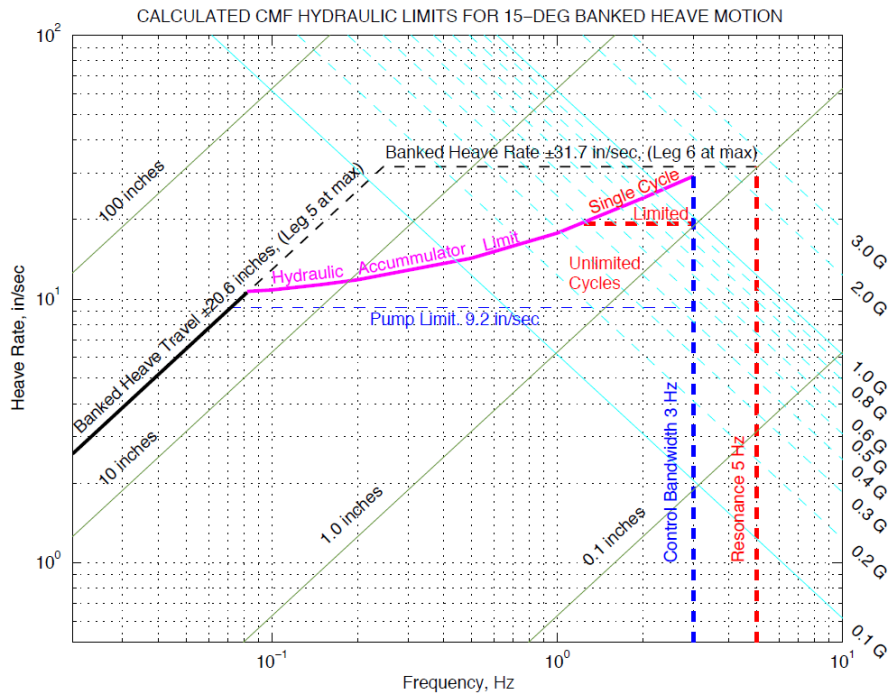


Figure 26: Operational Limits (Banked Heave)

CMF STANDARDIZED TESTING PROTOCOL

This section details testing protocols and analysis tools to be used to periodically validate the motion dynamics of the Cockpit Motion Base. These tools are also intended to provide comparable performance characteristic definitions in the event of future CMF modifications. A standard set of sinusoidal inputs for frequency domain analysis will be defined and described. Testing protocols using the CMF Host Test Interface to drive the motion base with sinusoidal signals will be introduced. Processing scripts, written in MATLAB and designed to illustrate the performance in a consistent manner, will be described. The performance results can be compared with past CM B/GFD performance data for periodic validation of proper performance or clear evaluation of performance improvement.

Standard Spectral Inputs

Frequency sweeps and banked sinusoidal acceleration commands are used for motion validation and are available as comma separated value (.csv) files.

Chirp Inputs

The frequency sweeps, or chirps, are used to generate Bode plots with information on the dynamic response of the motion base from its nominal orientation – defined as the position of the motion base at the completion of its “hold” state in the DCU. The frequency sweeps are available for all 6 simulator reference frame DoF. As discussed earlier, the frequency sweep was designed to minimize unnecessary violent accelerations on the system across the tested frequency ranges.

Banked, Sinusoidal Inputs

The banked, sinusoidal signals are used to assess the uncommanded acceleration in the lateral axis as a result of commanded vertical accelerations. This signal consists of four cycles of constant-frequency sinusoids ranging from 1Hz to 5Hz, in increments of 0.5Hz, splined together with simulator reference frame angular offsets from 0° to 13.5°, in 1.5° increments in the cab's roll-axis.

The input file commands translational displacements in inches and rotational displacements in radians. The commands are inertial/earth axes, NOT cab-axes. Therefore the input files will command the necessary combination of inertial axis heave and sway position to achieve pure, simulator reference frame heave commands when the cab is banked. This movement of combined sway and heave was coined as 'sweave'. More simply put, when the cab is rolled and pure heave is commanded in the simulator reference frame, the required input is combined sway and heave inertially. Figure 27 shows how this type of input looks in simulator reference frame. The bottom subplot is a zoomed-in snapshot of the 20 second splined segments seen in the top subplot.

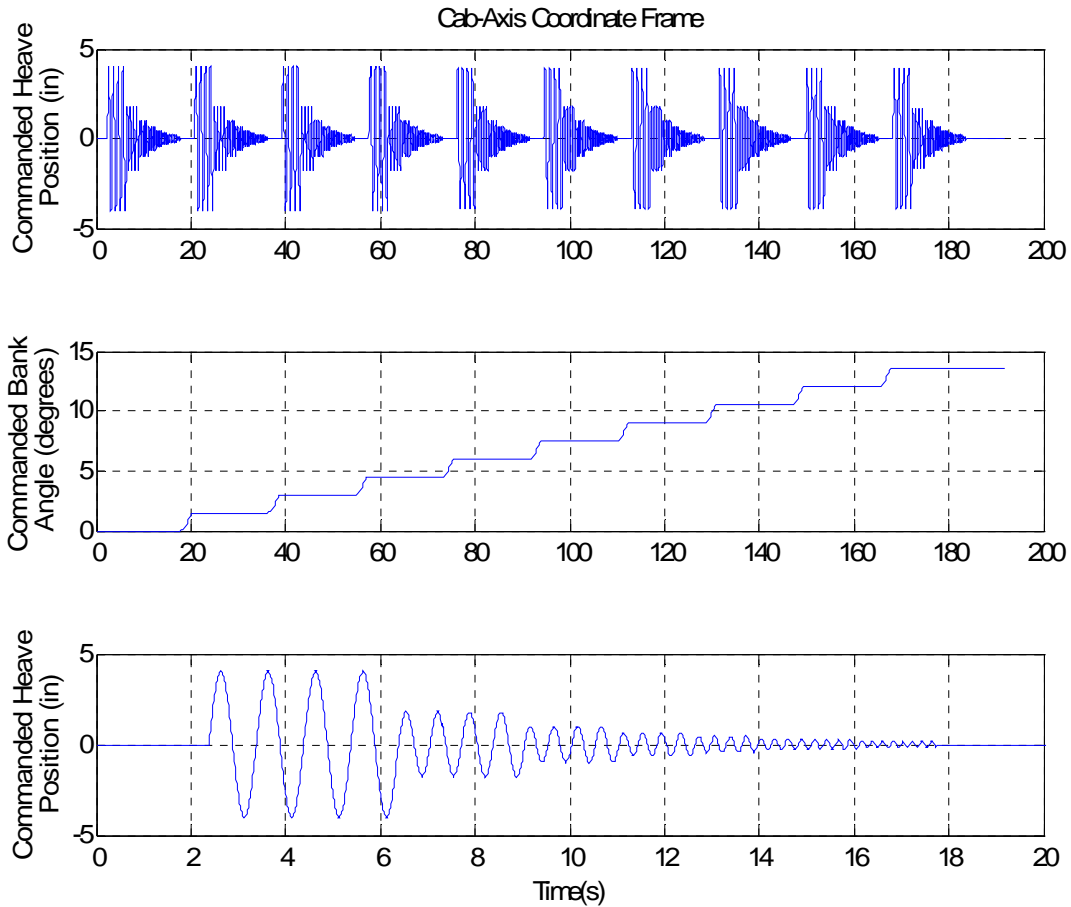


Figure 27: Sample sweave-spline time history

Standard Test Procedure

The provided test signals must be commanded via the host test interface at 100Hz. Six frequency sweep files are provided, for evaluation of all 6DoFs of the CMB. Two banked, sinusoidal signals are provided for evaluation of the uncommanded lateral acceleration in with left and right angular offsets. DVS data must be recorded for all runs so that it can be used for post-processing.

The GFD is the recommended cab for testing as the post-processing tools will provide an immediate comparison with past GFD data, however the RFD or the IFD can also be used.

Standard Post-Processing Tools

Automated Processing Scripts

Two post-processing scripts will generate a majority the results in this report for comparison of the current motion base performance to any future updates or retesting after calibrations. There is a 'readme.txt' file with basic instructions and descriptions provided with the software toolset.

Chirp Analyzer User Steps

1. Add the folder containing your DVS files of the frequency sweeps to your MATLAB path. This can be done within MATLAB by clicking "File" → "Set Path" and browsing to the directory in the resulting pop-up window.
2. Change MATLAB directory to the folder in which the 'ChirpAnalyzer.m' script is located.
3. Open 'ChirpAnalyzer.m' editor file.
4. Declare the filenames of the six DVS output files from the frequency sweeps and save the m.file.
5. Click "Run"

Graphical User Interface (GUI)

GUI User Steps

1. Repeat Step 1 from Section 0.
2. Change MATLAB directory to the folder in which SDAB_GUIv1 is located (... \Post Processing Scripts\SDAB GUI).
3. Open SDAB_GUIv1.m.
4. Run SDAB_GUIv1.m.
5. Click "Load DVS DATA" (once).
6. Use pop window to select the desired DVS output data file for plotting analysis. Note: You may need to specify "All Files" in the "Files of Type" drop down menu to see a .csv file. This data will take approximately a minute to load into the GUI.
7. Click on a parameter to the left to plot.
8. Change plot settings via button panels on the right.

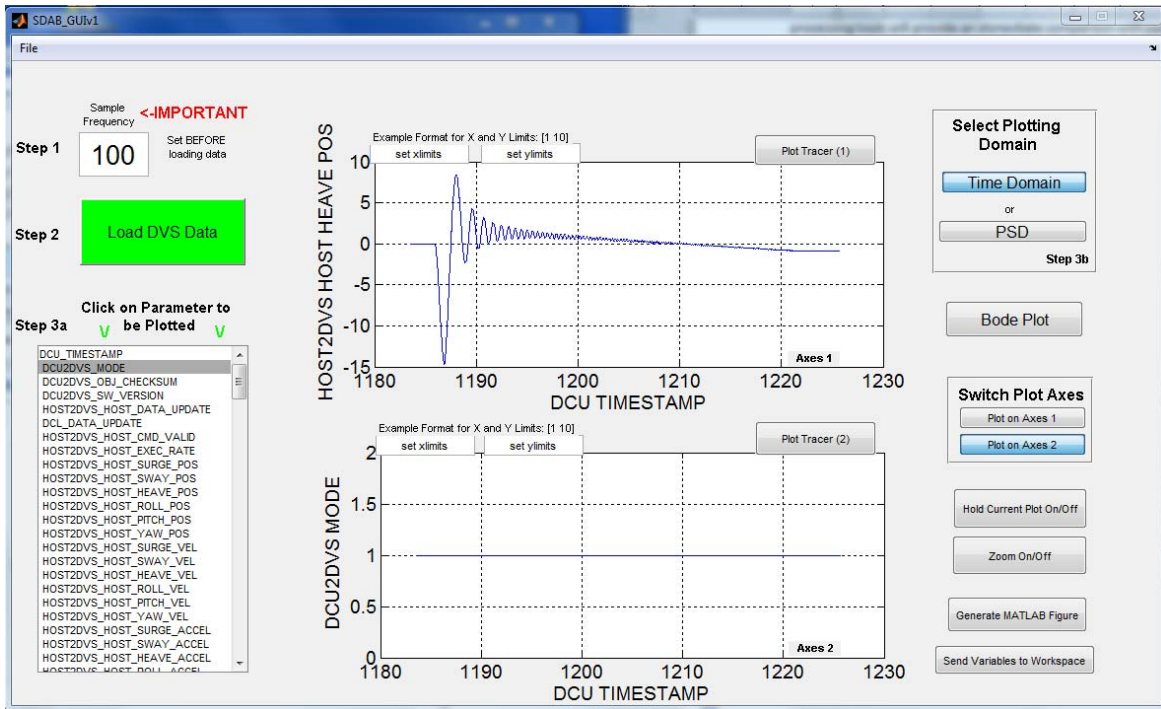


Figure 28: GUI - Post Processing Tool

Additional Functions

‘bode_plot’ – Plots the Power Spectral Density or Bode plot of the time domain signals sampled at the specified sampling frequency

‘plotter’ - Plotting function called by various several scripts

CONSIDERATIONS

Future improvements may be realizable from both software and hardware modifications. The following areas of improvement are briefly introduced for awareness only.

The nature of the parasitic acceleration demonstrates repeatability and linear relationships with increasing frequency of commanded accelerations. The control law could potentially be revised to include a feed-forward correction from a model of the measured parasitic accelerations. This and other control law improvements are continuously under evaluation by the SDAB.

Several modifications to the hardware could also potentially lead to improved bandwidth and reductions in parasitic acceleration. A large catwalk was added to the platform for accessibility which ultimately adds a large mass at a long lever arm from the centroid of the platform. Any reduction or the entire removal of the platform would likely result in a quantifiable improvement in motion bandwidth and likely parasitic acceleration.

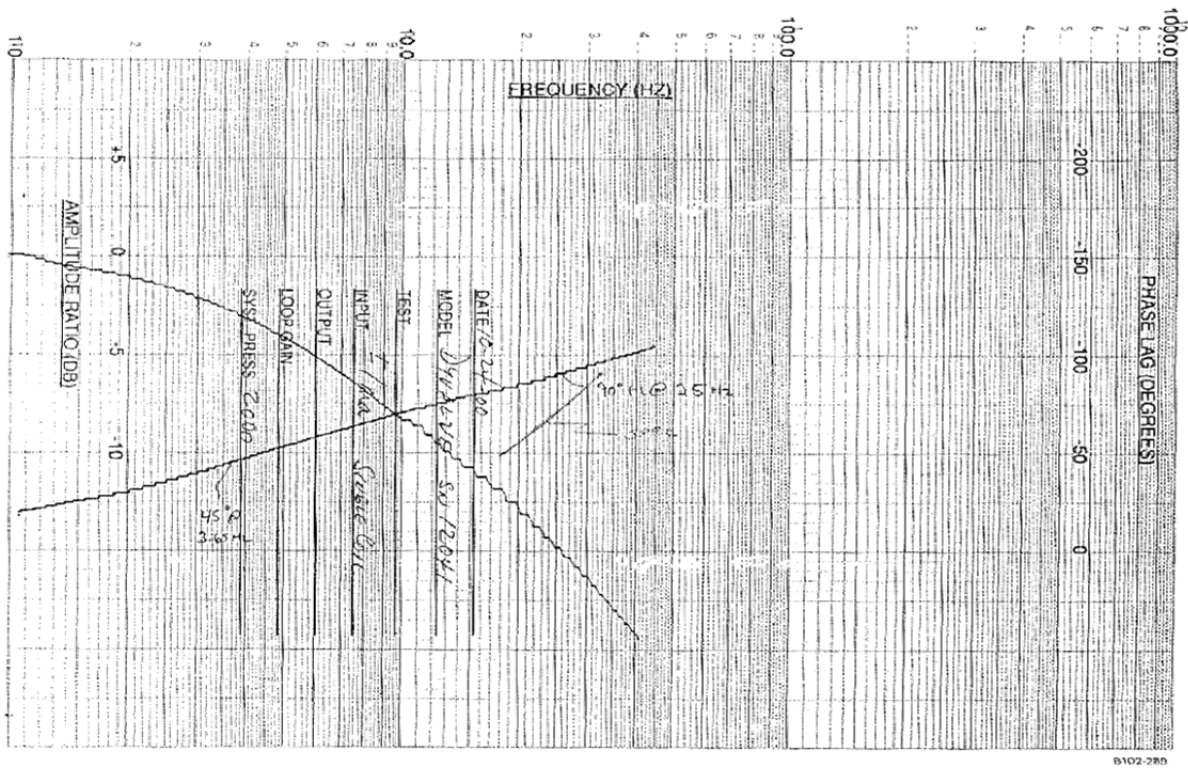


Figure 29: CMB valve performance

Valve performance from a testbed assessment indicates a current valve bandwidth of <4 Hz at 45°. The results of this test are presented in Figure 29. Increasing pump capacity may provide an opportunity to further increase motion bandwidth and allow for more control authority to further reduce parasitic acceleration. Quantification of such improvements is also currently under evaluation by the SDAB.

CONCLUSIONS

The current, closed-loop performance of the CMB/GFD was presented as it exists with the production control law. The new production controller showed a clear reduction in parasitic acceleration with minimal impact to closed-loop performance. Operational limits characterizing the motion envelope were documented. This performance characterization is a vital tool for future researchers and experiments requiring accurate replication of commanded motion. The standardized testing protocol allows for the reproduction of these results in a consistent manner for periodic re-evaluation of the CMB as well as after any future system modifications, both hardware and software.

BIBLIOGRAPHY

- [1] B. R. Bryant, CMF Motion Base Control System Derived Requirements. Version A., Hampton, VA: NASA Langley Research Center. Airbone Systems Competency. Systems and Development Branch, February 5, 2001.
- [2] "Dynamic Characteristics of Flight Simulator Motion Systems," Advisory Group for Aerospace Research and Development, North Atlantic Treaty Organization, number AGARD-AR-144, AGARD Advisory Report, 1979
- [3] B. N. Tomlinson, "Simulator Motion Characteristics and Perceptual Fidelity, A Progress Report," AGARD Conference Proceedings Number 408, Flight Simulation, 7 Rue Ancelle, 922200 Neuilly sur Seine, France, pages 6A-1--6A-12, Advisory Group for Aerospace Research and Development, North Atlantic Treaty Organization, 1986.
- [4] Robert J. Telban, Weimin Wu and Frank M. Cardullo, Motion Cueing Algorithm Development: Initial Investigation and Redesign of the Algorithms, NASA Langley Research Center, Hampton (VA), number NASA-CR-2000-209863, Contractor Report, 2000.
- [5] L. Gupton, PRT for GFD Motion Shakedown (Test Plans 3.1 - 3.5 and 3.10). Safety Interlocks and DOF Performance Evaluation, October 6, 2008.
- [6] W.R. Berkouwer, O. Stroosma, M.M. van Paassen, M. Mulder and J.A. Mulder, "Measuring the Performance of the SIMONA Research Simulator's Motion System," Proceedings of the AIAA Modeling and Simulation Technologies Conference, San Francisco, California, Aug. 15-18, 2005.
- [7] P. M. T. Zaal, F. M. Nieuwenhuizen, M. Mulder and M. M. van Paassen, "Maximum Likelihood Estimation of Multi-Modal Pilot Control Behavior in a Target-Following Task," IEEE International Conference on Systems, Man and Cybernetics, Singapore, Oct. 12-15 2008.
- [8] Mathworks, "R2012a Documentation -> DSP System Toolbox -> Blocks -> Sources -> "Chirp"," Mathworks. Product Documentation., 2012.
- [9] L. E. Gupton, R. B. Bryant and D. J. Carrilli, "Evaluating the Performance of the NASA LARC CMF Motion Base Safety Devices," Proceedings of the AIAA Modeling and Simulation Technologies Conference, Keystone, Colorado, August 21-24, 2006.
- [10] "Integrated Intelligent Flight Deck Technologies (2006-2010). Facilities: Cockpit Motion Facility (CMF)," [Online]. Available: <http://www.aeronautics.nasa.gov/avsafe/iifd/cmf.htm>. [Accessed 08 August 2012].

APPENDIX

Comparison of Production Controller to Previous Controller

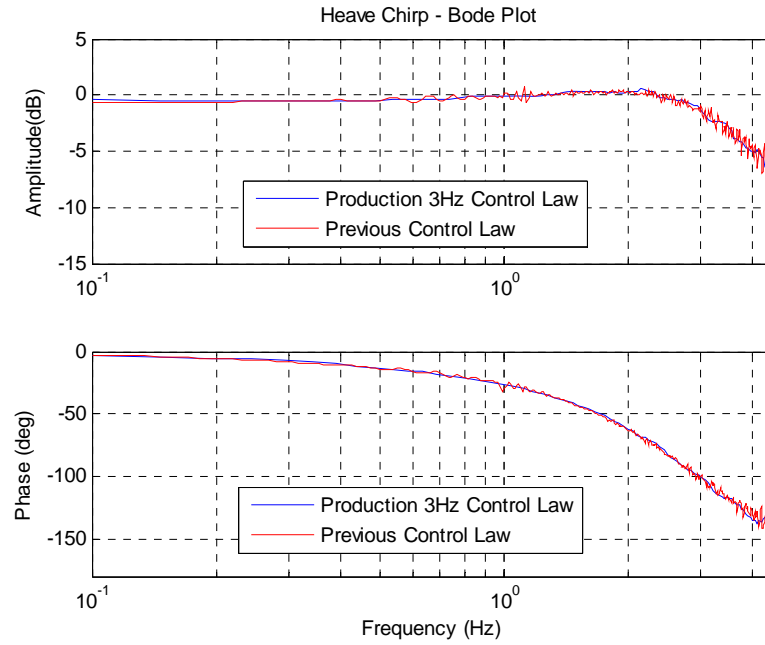


Figure 30: Bode Plot Comparison – Heave

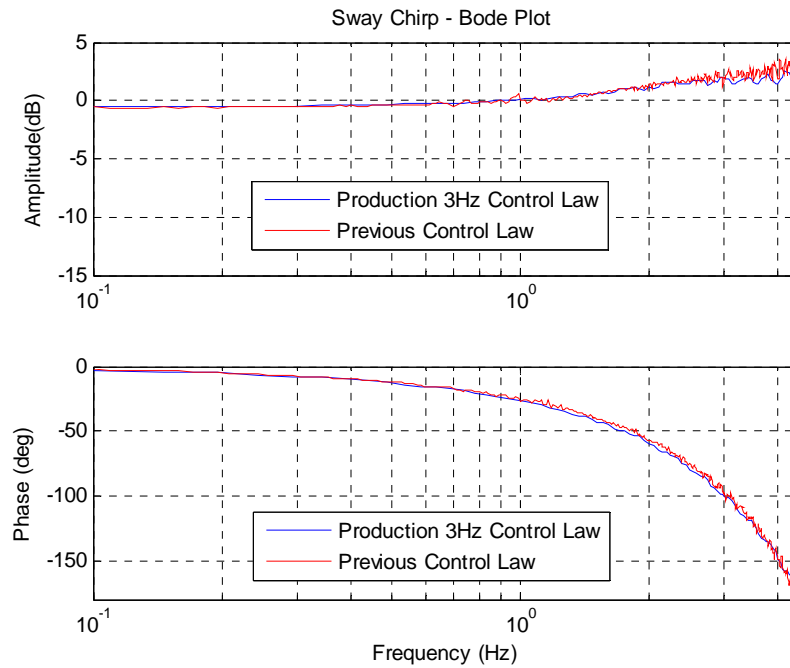


Figure 31: Bode Plot Comparison – Sway

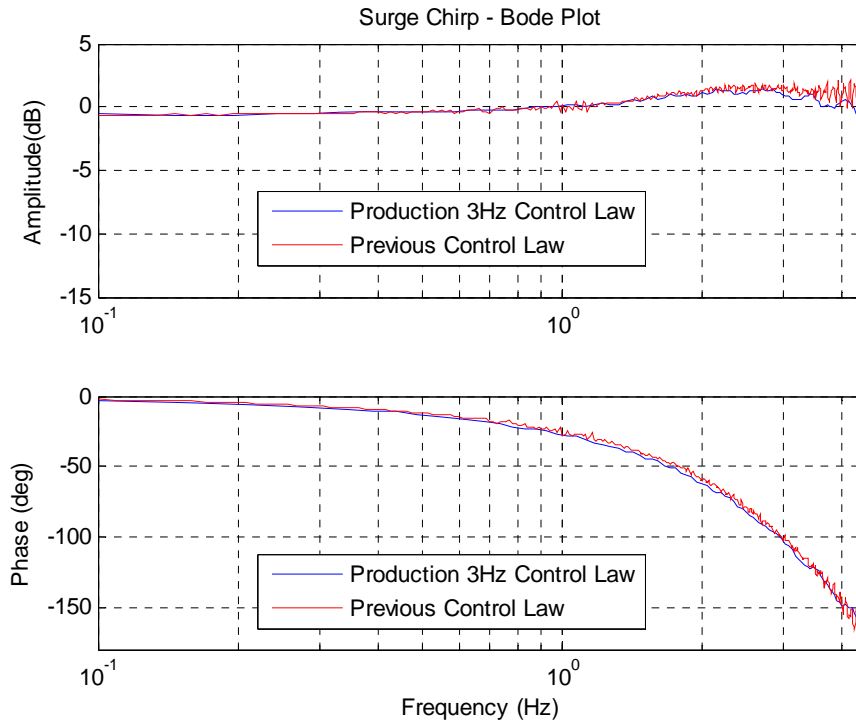


Figure 32: Bode Plot Comparison – Surge

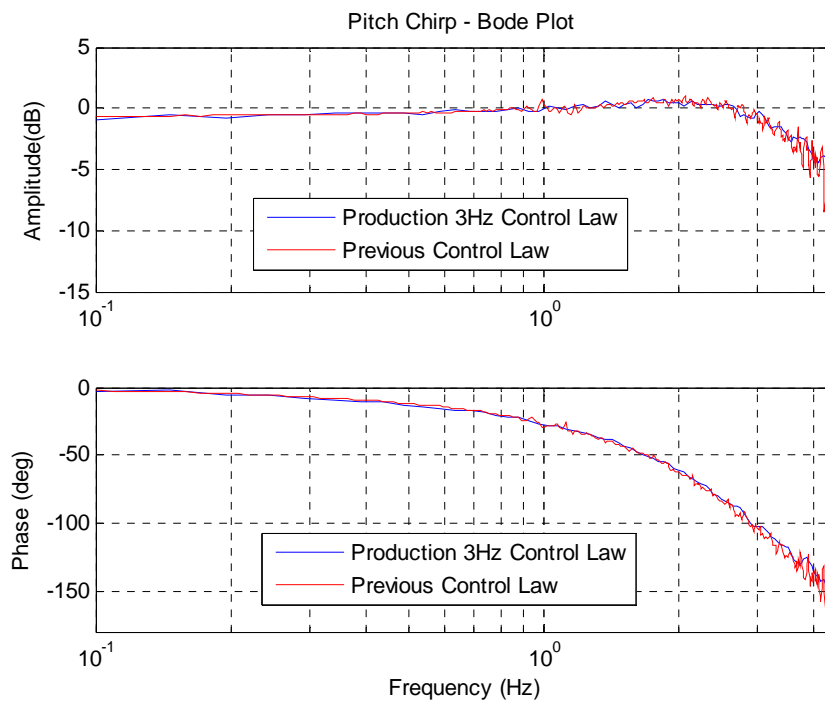


Figure 33: Bode Plot Comparison – Pitch

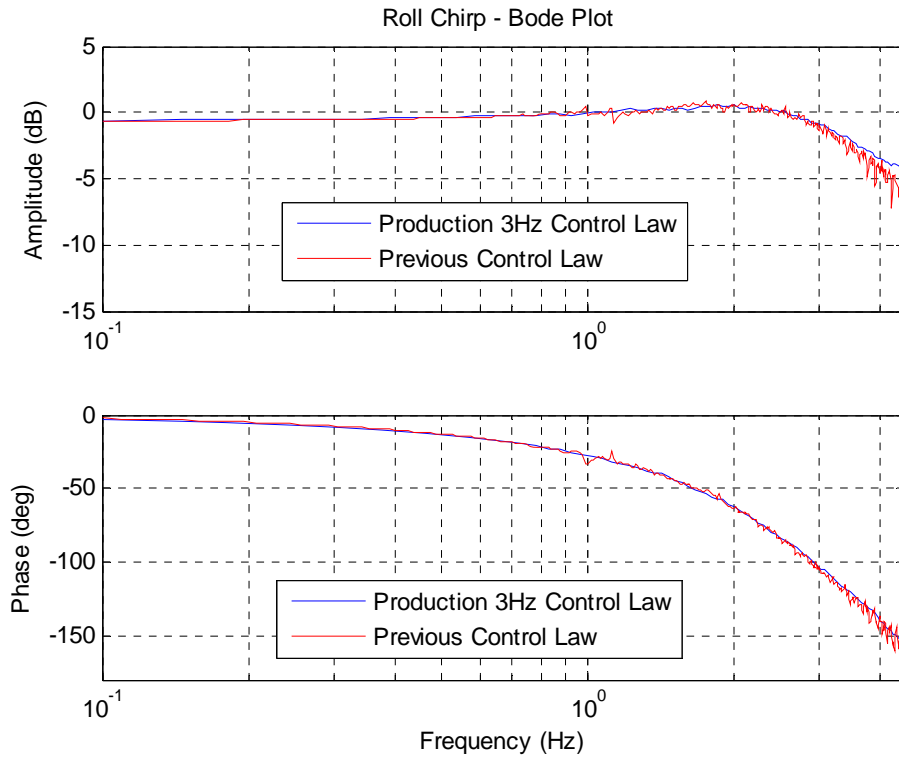


Figure 34: Bode Plot Comparison – Roll

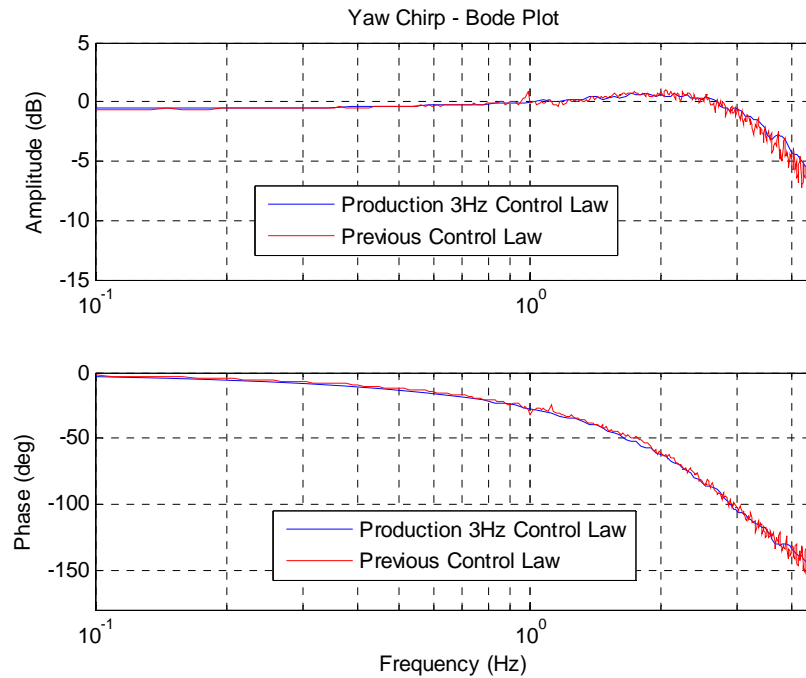


Figure 35: Bode Plot Comparison – Yaw

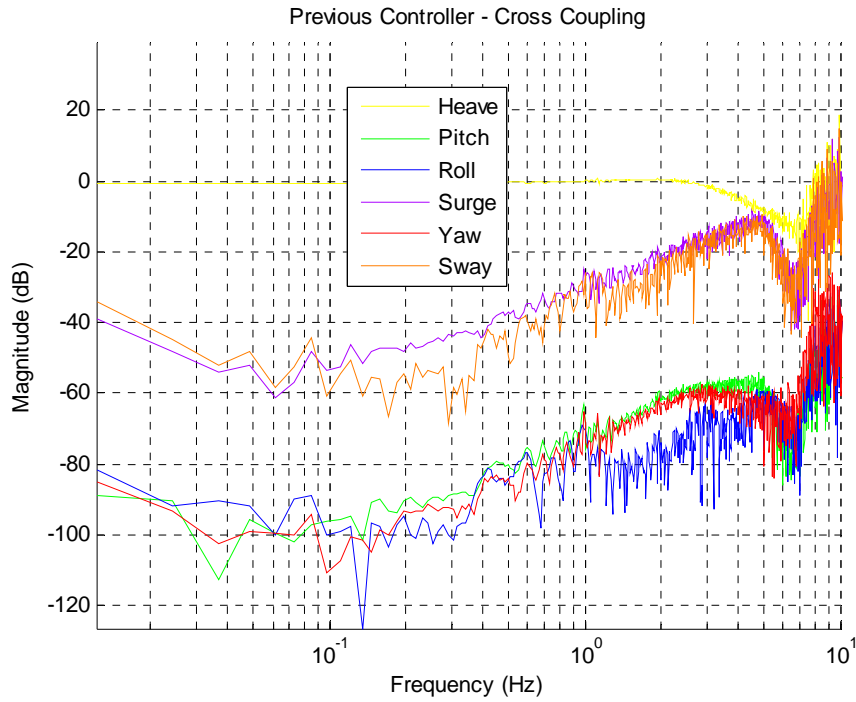


Figure 36: Previous Controller - Parasitic Acceleration from Commanded Heave (dB)

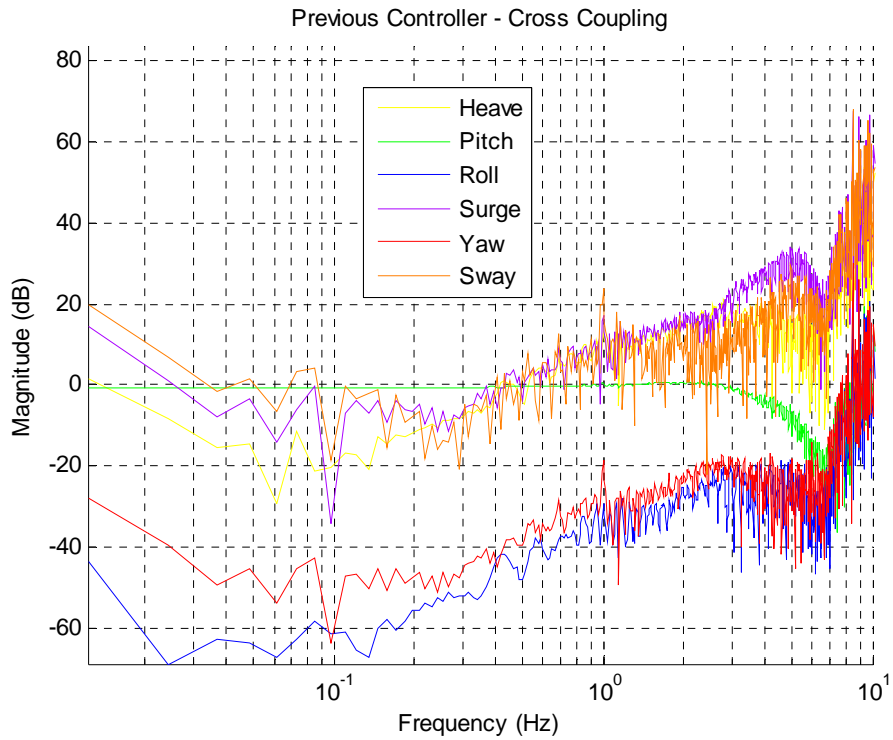


Figure 37: Previous Controller - Parasitic Acceleration from Commanded Pitch (dB)

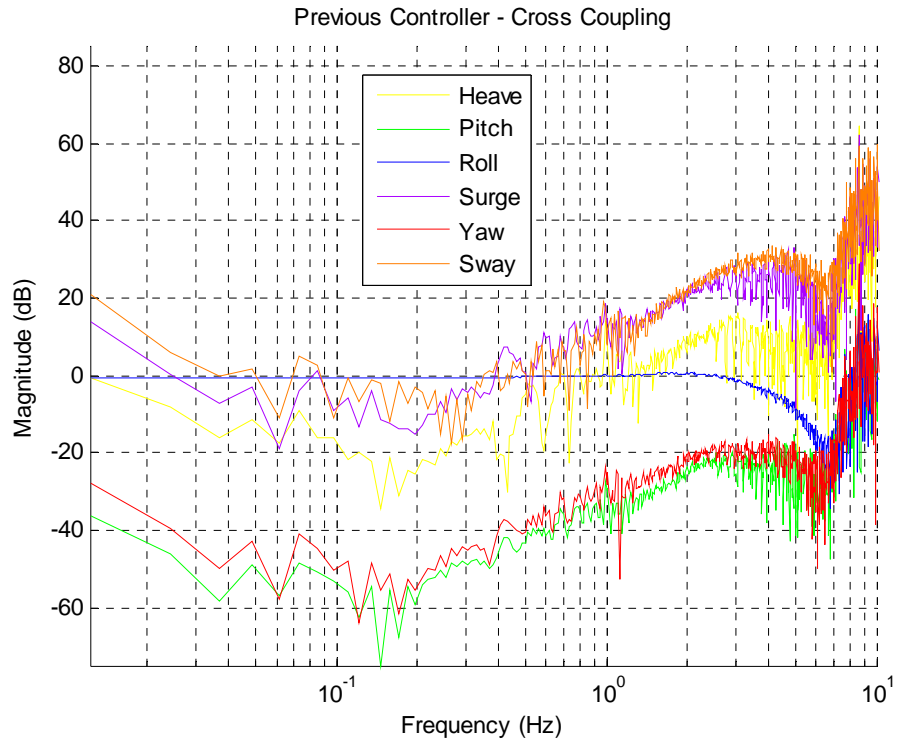


Figure 38: Previous Controller - Parasitic Acceleration from Commanded Roll (dB)

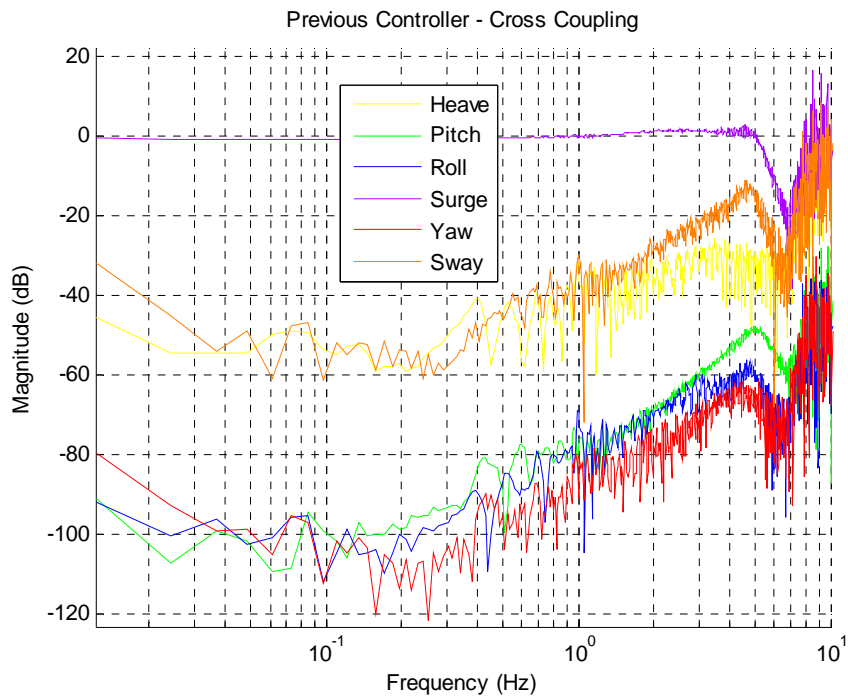


Figure 39: Previous Controller - Parasitic Acceleration from Commanded Surge (dB)

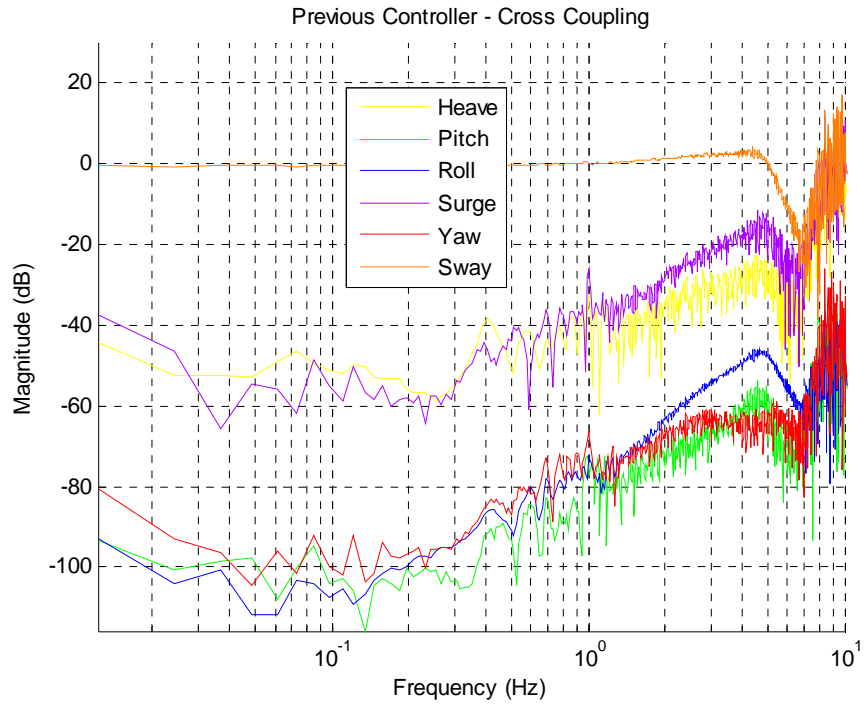


Figure 40: Previous Controller - Parasitic Acceleration from Commanded Sway (dB)

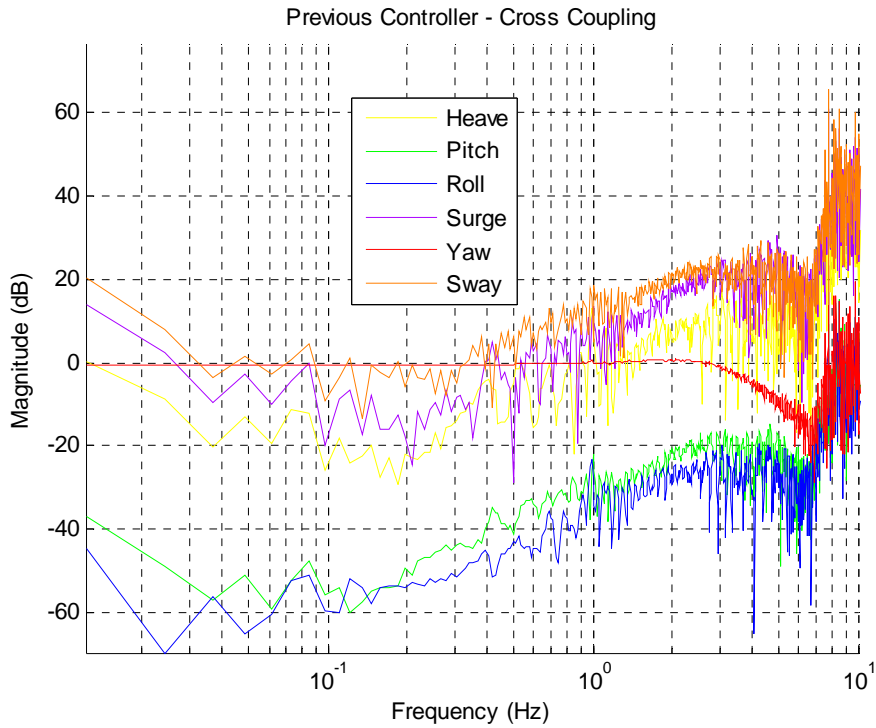


Figure 41: Previous Controller - Parasitic Acceleration from Commanded Yaw (dB)

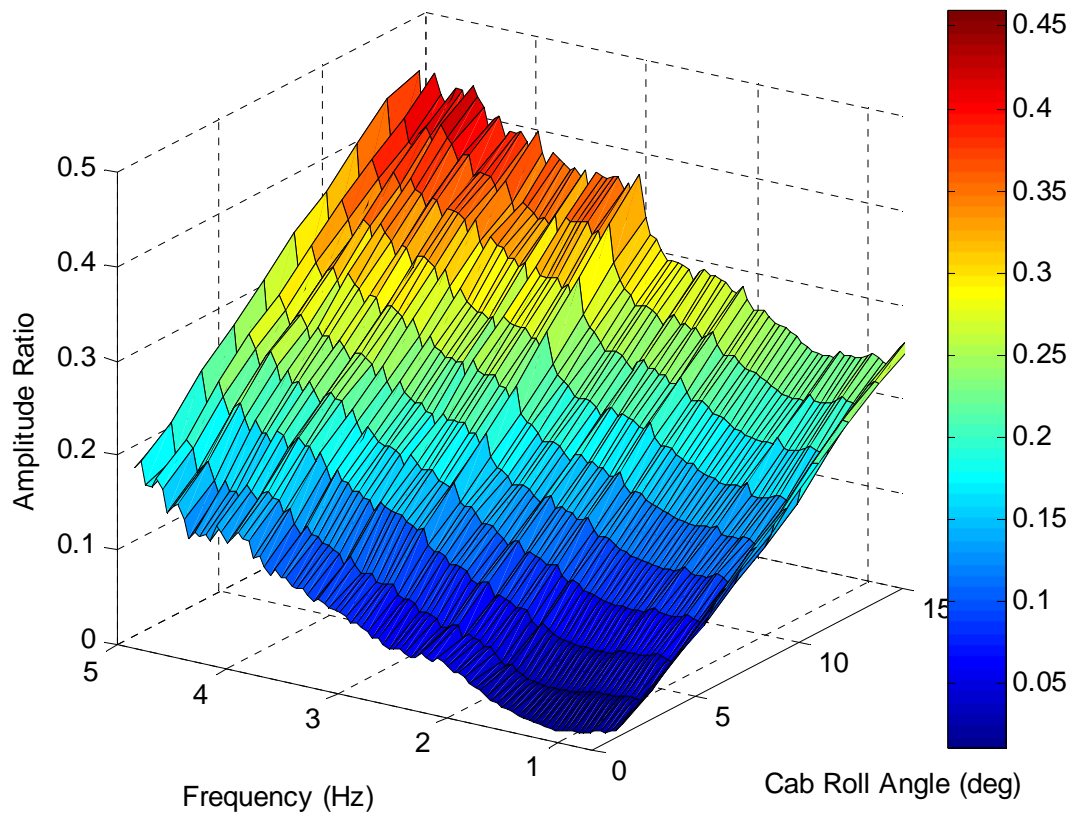


Figure 42: Previous Controller – Cross-coupled acceleration gains by increasing cab roll angle

REPORT DOCUMENTATION PAGE

*Form Approved
OMB No. 0704-0188*

The public reporting burden for this collection of information is estimated to average 1 hour per response, including the time for reviewing instructions, searching existing data sources, gathering and maintaining the data needed, and completing and reviewing the collection of information. Send comments regarding this burden estimate or any other aspect of this collection of information, including suggestions for reducing this burden, to Department of Defense, Washington Headquarters Services, Directorate for Information Operations and Reports (0704-0188), 1215 Jefferson Davis Highway, Suite 1204, Arlington, VA 22202-4302. Respondents should be aware that notwithstanding any other provision of law, no person shall be subject to any penalty for failing to comply with a collection of information if it does not display a currently valid OMB control number.
PLEASE DO NOT RETURN YOUR FORM TO THE ABOVE ADDRESS.

1. REPORT DATE (DD-MM-YYYY) 01-01 - 2014		2. REPORT TYPE Technical Memorandum		3. DATES COVERED (From - To)	
4. TITLE AND SUBTITLE Current Performance Characteristics of NASA Langley Research Center's Cockpit Motion Base and Standardized Test Procedure for Future Performance Characterization				5a. CONTRACT NUMBER	
				5b. GRANT NUMBER	
				5c. PROGRAM ELEMENT NUMBER	
				5d. PROJECT NUMBER	
6. AUTHOR(S) Cowen, Brandon; Stringer, Mary T.; Hutchinson, Brian K.; Davidson, Paul C.; Gupton, Lawrence E.				5e. TASK NUMBER	
				5f. WORK UNIT NUMBER 160961.01.02.01	
				8. PERFORMING ORGANIZATION REPORT NUMBER L-20355	
7. PERFORMING ORGANIZATION NAME(S) AND ADDRESS(ES) NASA Langley Research Center Hampton, VA 23681-2199				10. SPONSOR/MONITOR'S ACRONYM(S) NASA	
9. SPONSORING/MONITORING AGENCY NAME(S) AND ADDRESS(ES) National Aeronautics and Space Administration Washington, DC 20546-0001				11. SPONSOR/MONITOR'S REPORT NUMBER(S) NASA/TM-2014-218148	
12. DISTRIBUTION/AVAILABILITY STATEMENT Unclassified - Unlimited Subject Category 12 Availability: NASA CASI (443) 757-5802					
13. SUPPLEMENTARY NOTES					
14. ABSTRACT This report documents the updated performance characteristics of NASA Langley Research Center's (LaRC) Cockpit Motion Base (CMB) after recent revisions that were made to its inner-loop, feedback control law. The modifications to the control law will be briefly described. The performance of the Cockpit Motion Facility (CMF) will be presented. A short graphical comparison to the previous control law can be found in the appendix of this report. The revised controller will be shown to yield reduced parasitic accelerations with respect to the previous controller. Metrics based on the AGARD Advisory Report No. 144 are used to assess the overall system performance due to its recent control algorithm modification. This report also documents the standardized simulator test procedure which can be used in the future to evaluate potential updates to the control law.					
15. SUBJECT TERMS Control Theory; Motion Base; Simulation					
16. SECURITY CLASSIFICATION OF:			17. LIMITATION OF ABSTRACT	18. NUMBER OF PAGES	19a. NAME OF RESPONSIBLE PERSON
a. REPORT	b. ABSTRACT	c. THIS PAGE			STI Help Desk (email: help@sti.nasa.gov)
U	U	U	UU	42	19b. TELEPHONE NUMBER (Include area code) (443) 757-5802